1970

The evaluation of radar guided missile performance using various target glint models

Franklin Delano Hockett

Department:

THE EVALUATION OF RADAR GUIDED MISSILE PERFORMANCE USING VARIOUS TARGET GLINT MODELS

BY

FRANKLIN DELANO HOCKETT, 1933

A

THESIS

submitted to the faculty of

THE UNIVERSITY OF MISSOURI - ROLLA

in partial fulfillment of the requirements for the

Degree of

MASTER OF SCIENCE IN ELECTRICAL ENGINEERING

Rolla, Missouri

1970

Approved by

(advisor)

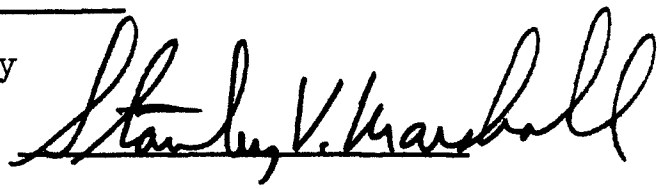

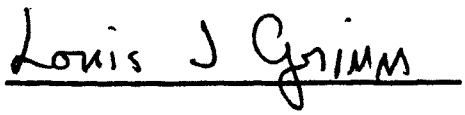

_____

ABSTRACT

A radar guided missile seeker approaching a target arrives at a crossover point beyond which the entire target is illuminated by the missile seeker's radar antenna beam. When this occurs, for a complex target, the radar senses a time changing target center location which may greatly complicate the terminal tracking portion of the seeker's flight. This thesis documents various glint models in use today and compares the performance of these models by using a seeker model to determine the effect of glint on terminal tracking performance.

A large volume of data has been compiled describing various radar characteristics of complex targets. Some of the glint models discussed herein are the result of independent investigations and some models are derived analytically. The return energy transmitted from a radar and reflected from a complex target is generally statistical in nature due to the random nature of the reflecting surfaces dispersed over the target vehicle and also because the target is continually changing aspect.

A radar target's reflecting characteristics are of concern when a seeker is attempting to acquire the target and again when the seeker is closing on the target. A

large amount of data exists for determining long range acquisition capabilities of various radar schemes.

The acquisition of a target in a sea clutter background has been thoroughly investigated in the past decade and today's improved techniques (Moving Target Indication and Pulse Compression) have enabled moderately powered radars to acquire very small targets in high sea states. At long ranges, the individual target elements present a unified amplitude response (or appear as a point source). The main problem during acquisition is to reduce the viewing area to dimensions comparable to the target so that the target return will be distinguishable. This argument does not apply to an interferometer as target phase variations will still contribute to acquisition error, however the sophistication required to implement interferometers into a seeker design precludes their use for present day tracking schemes.

Although acquisition problems can severely limit the response time of a seeker bearing vehicle or aircraft to an eminent attack threat, the inability of a radar seeker to operate in the presence of angle glint can render the seeker useless. A seeker's design must often be a compromise between tracking accuracy, acquisition capability, and dynamic versatility, since the weight and cost penalties associated with multiple radar tracking modes within a single seeker are prohibitive.

Therefore, since the literature abounds with acquisition theory and techniques, the main portion of this thesis consists of analyzing the post-acquisition seeker performance in the presence of angular glint or angle noise.

The glint models used in this analysis represent models in use at the present time. In addition, models which were derived are compared to determine the degree of correlation which exists between measured target models and those models which are derived from their statistical characteristics. The method employed for the evaluation is general in nature so that the procedure could be used to evaluate any subsequent glint model derivations. In addition, some recent work is summarized which demonstrates the advantages of using swept frequency techniques to improve radar tracking performance in the presence of angular glint.

TABLE OF CONTENTS

Page

FIGURES

List of Symbols

S/N - IF Signal-to-Noise Ratio

P_t - Transmitted Power

G_a - Antenna Gain

λ - Wavelength

R - Radar Range

K - Boltzmann's Constant

κ - Constant (general)

σ - Radar Cross Section

T - Absolute Temperature

B - Receiver Noise Bandwidth

$\dot{\gamma}$ - Missile Velocity Vector

A_{LS} - Line-of-Sight Angle

$\dot{A}_{LS}$ - Line-of-Sight Rate

A_{TL} - Antenna Angle

G_1 - Radar Shaping Network

G_2 - Radar Amplifier, power amplifier, and actuator antenna Gimbal

V_R - Rate Command

Θ - Disturbance Input

K_G - Gain of the Gyro Feedback Path

s, S - LaPlace Transform Variable

ω - Angular Frequency Variable

E_T - Tracking Error

K_P - Position error coefficient

K_V - Velocity error coefficient

K_a - Acceleration error coefficient

$\dot{A}_{TL}$ - Time Derivative of antenna angle

θ' - Time Derivative of input disturbance

θ_o - Radar antenna crossover point on receiver antenna base line

α_i - Relative phase difference for the returned signals from multi-reflector targets

a_i - Ratio of target amplitudes

e_N - Individual reflector's (target) amplitude

θ_{T_i} - Target Angular coordinates

P_i - Incident power

$\bar{E}$ - Electric field strength vector

$\bar{H}$ - Magnetic field strength vector

η - Intrinsic impedance

d_k - Distance of elemental target reflectors from receiver

$\bar{E}_{rk}$ - The reflected field produced by the k^{th} target element

n - Number of independent target elements

ω_g - Half-power frequency (noise bandwidth)

ω_a - Rate of change of aspect angle

L - Maximum dimension of the target

$\phi(0)$ - Zero frequency spectral density

σ_i - Standard deviation of a statistical distribution

M_i - Mean of a statistical distribution

ℓ - Loss Factor

NF_0 - Receiver noise figure

I. INTRODUCTION

During the past decade, a considerable amount of effort has been expended in perfecting existing radar techniques. The radar industry has been saturated with new circuit and system techniques. The art of control dynamics has been perfected to the extent that an enormous volume of material exists describing the application of these methods to various types of controlled vehicles. New and more sophisticated transmitting and receiving devices have been introduced into the radar industry. The radar industry has reached a high level of maturity in developing radar equipment of all description and for many various applications.

The largest problem which confronts the radar system designed is that of being able to adequately describe the radar's operating environment and its effect on radar performance. In addition, the radar designer must be capable of deriving radar cross sections which will be an adequate basis for radar design.

For the present discussion, the radar application is that where a radar is used to assist a missile in acquiring a target and then tracking the target to the point where the missile proximity fuse will dispose of the target (for the purposes of discussion in this article it will be assumed that the missile will impact with the

target - although this is not a necessary condition for successful missile performance).

Two primary areas of interest for an air launched anti-ship missile are the background clutter from which a ship (or target in general) must be detected (a long range effect) and the disturbing influence of angular glint on the seeker's tracking characteristics (a short range effect). A ship will be used for the analysis of this paper since the problems associated with a moving target are best illustrated by a conservative target estimate. A more dynamic situation would be the interception of an aircraft with a missile seeker, however, the increased analytic complexity does not seem warranted since the basic technique, not all of the potential applications, is the intended goal of the paper.

The problem of clutter has received a great deal of attention in the literature. Nevertheless, acquisition represents a very important phase of a modern anti-ship weapon system since the response time of an attacking aircraft equipped with missile seekers is related to the ability of the seeker to lock on the target. In addition, the more favorable logistics of increased range acquisition handicaps a potential enemy in detecting and locating the carrier aircraft.

Although less frequently discussed, the problems associated with angular glint can be much more damaging and generally increase the design difficulties. At large ranges, assuming acquisition has taken place, the target can be assumed to be a point source and the well known radar equation can be used. For non-cooperative tracking (using reflected energy) the relationship for the IF (Intermediate Frequency) signal-to-noise is given by[1] as:

$$S/N = \frac{P_t G^2 \lambda^2 \sigma}{(4\pi)^3 R^4 K T_0 B N F_0 \ell}$$

where S/N is the receiver signal-to-noise ratio prior to envelope detection but after IF amplification

P_t is the transmitted power in watts

G is the antenna gain (this assumes the same antenna is used for receiving and transmitting)

λ is the radar wavelength in consistent units

σ is the radar cross section in consistent units

R is the Radar Range in consistent units

K is Boltzmann's constant 1.38×10^{-23} watts per hertz per degree kelvin

T is the absolute temperature of the signal source in degrees kelvin

B is the equivalent noise bandwidth of the receiver in hertz

ℓ Loss factor, numeric

NF_0 Receiver Noise figure, numeric

The radar cross section term, σ, is the most difficult term in the radar equation to describe analytically. For relatively simple geometries, analytic solutions can be obtained and these are listed in reference 1. For more complicated targets either a physical model must be constructed and evaluated using an antenna range or a mathematical model must be derived. In either case, some means is required to determine the effect of the target cross section variation on radar performance.

Now assume the target is being tracked. A thorough discussion of acquisition techniques can be found in either reference 1 or 2. As the range to the target decreases glint becomes more pronounced. The critical point of the missile flight path (with respect to glint) occurs when the target subtends the tracking antenna beamwidth and small variations in pointing commands at this range represent large disturbances to the missile (vehicles) control dynamics. A definition of angular glint is given by[1] as: "The disturbance in apparent angle of arrival due to interference phenomena between reflecting elements of the target." Therefore, the degree of success in designing a missile seeker depends to a large degree on the systems engineer's ability to determine the glint spectrum for the anticipated target vehicles. Here again, where exact surface features are

known (a condition not likely to exist for non-cooperative targets) a physical model will provide a good basis for determining the glint spectrum. Where this data is missing, one has to either use similar target characteristics or provide a mathematical model sufficiently similar in large dimensions to provide the required data. For a target with any complexity the analytic method must use a statistical approach.

The final step in this analysis is to provide a comparative basis from which design trade-offs can be made. To accomplish this a general seeker model will be used, and since the intent of this paper is not to design a missile seeker, a conventional seeker scheme will be used for comparison purposes. During the last three years frequency agile radars (swept frequency radars) have been used to increase the acquisition range and reduce the glint spectrum effect on tracking accuracy. A discussion of this new area of research is included.

II. SEEKER DESCRIPTION

A. General

Since the primary objective of this analysis is to derive a glint model, the radar model and control dynamics scheme were selected from an existing design described in reference [2]. This was done to prevent including a large amount of analytic detail which is present in a great number of periodicals and standard radar textbooks. Also, the final conclusions concerning the developed glint model can best be determined by comparisons made with existing models using a familar radar tracking scheme. The tracking scheme used is contained in chapter 9 of reference 2. Basically, the tracker design used will be a proportional navigation scheme. The dynamic equations for this seeker are developed in appendix I.*

The radar seeker steady-state error as influenced by the tracking loop bandwidth is analyzed for a point in the missile trajectory close to the target. The means by which the seeker arrived at this point (acquisition and inertial guidance) will not be dwelt on as this is another phase in the seeker designs where the effects of

---

*A brief description and the equations of motion are contained in appendix I.

receiver noise, clutter and general transmission quantities must be evaluated. The ultimate performance criterion for a radar seeker design in the application of a guided missile is the missile miss distance. However, the sensitivity of this parameter to various error sources requires that we consider the design of an entire radar seeker-autopilot-airframe flight dynamics loop, which is beyond the scope of this investigation. The discussion, therefore, is restricted to the analysis of errors in the rate commands generated by the seeker (which are supplied as an input to an autopilot in a proportional navigation scheme) as a function of line-of-sight variations.

B. Seeker Functional Description

Figure 1 is a diagram of the missile control system for one channel (azimuth or elevation) of a proportional navigation scheme. In such a scheme, the angular velocity of the missile's velocity vector, $\dot{\gamma}$*, is commanded proportional to the missile target line-of-sight rate; i.e. $\dot{\gamma} = q\dot{A}_{LS}$** where q is the constant of proportionality and $\dot{A}_{LS}$ is the line-of-sight rate. The seeker description of figure 1 encompasses the tracking and

---

*Characters dotted represent derivatives with respect to the appropriate independent variable.

**See equation AI-9, Appendix 1.

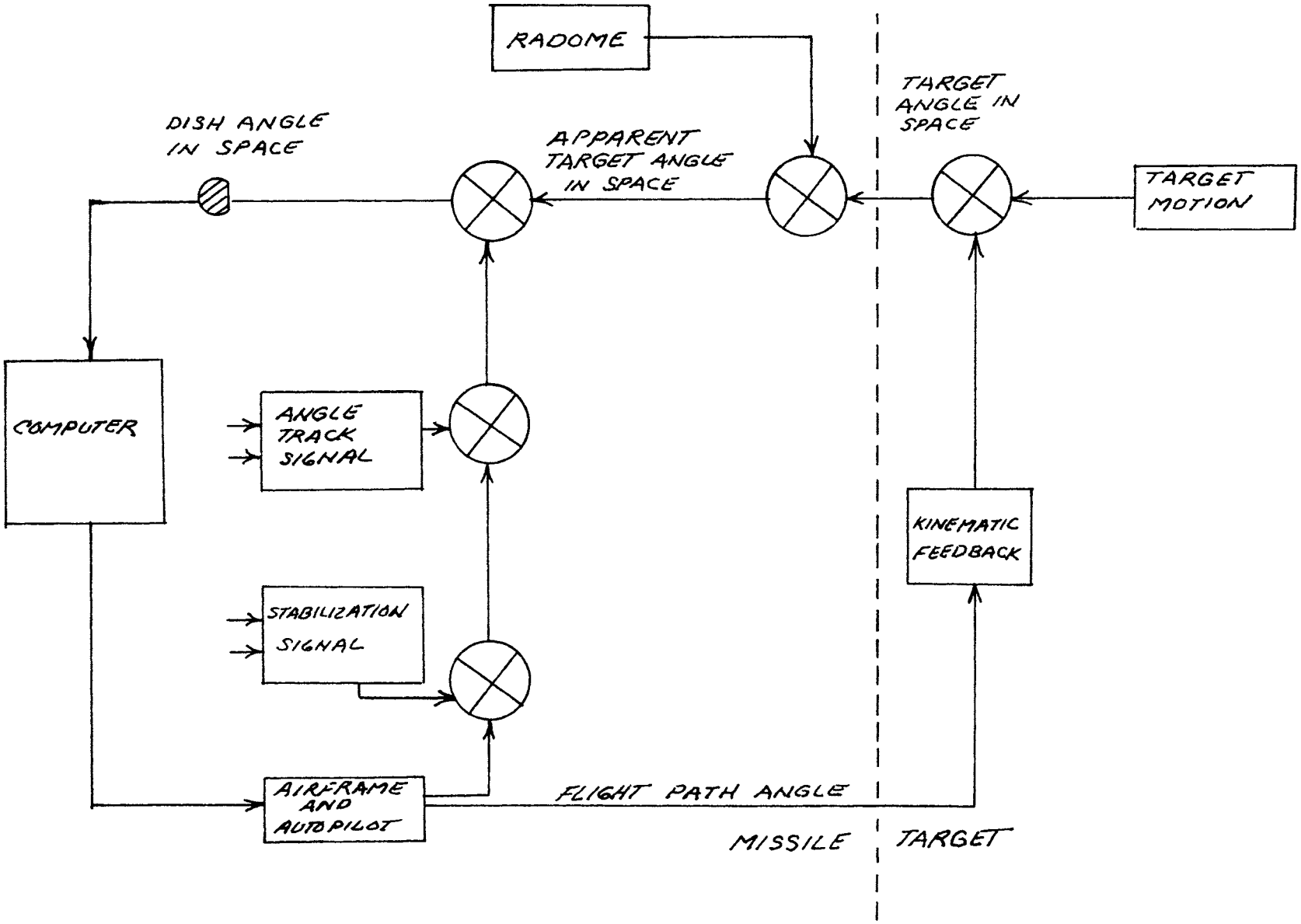

FIGURE II-1

GENERAL MISSILE GUIDANCE SYSTEM

stabilization loops. Generally speaking, glint produces the largest effect in the azimuth channel where the target aspect can be in the neighborhood of an order of magnitude greater than the elevation.

Now the radar seeker design must allow the seeker's antenna to remain pointed at the target during target or platform motion, however, the response must be slow enough to prohibit the seeker from responding to noise inputs to the radar receiver. Therefore, the seeker design represents a compromise whereby the loop response needed to reduce antenna platform motion is obtained with the stabilization loop, and the slower tracking loop is designed to provide noise filtering without causing large dynamic bias error. Figure (2) is a diagram giving simplified transfer functions of the variable components. The stabilization loop includes the antenna gimbal, gimbal actuator, and actuator drive amplifier, a rate gyro and shaping networks. Examination of the transfer function A_{TL}/θ indicates that a high loop gain is necessary to provide stabilization. For this situation the transfer function $\frac{A_{TL}}{V_R}$ is approximately $1/K_G S$ where K_G is the gain of the gyro feedback path. The tracking loop includes the radar receiver, the angle tracking demodulation, amplifier, bandwidth shaping circuits, and the stabilization loop

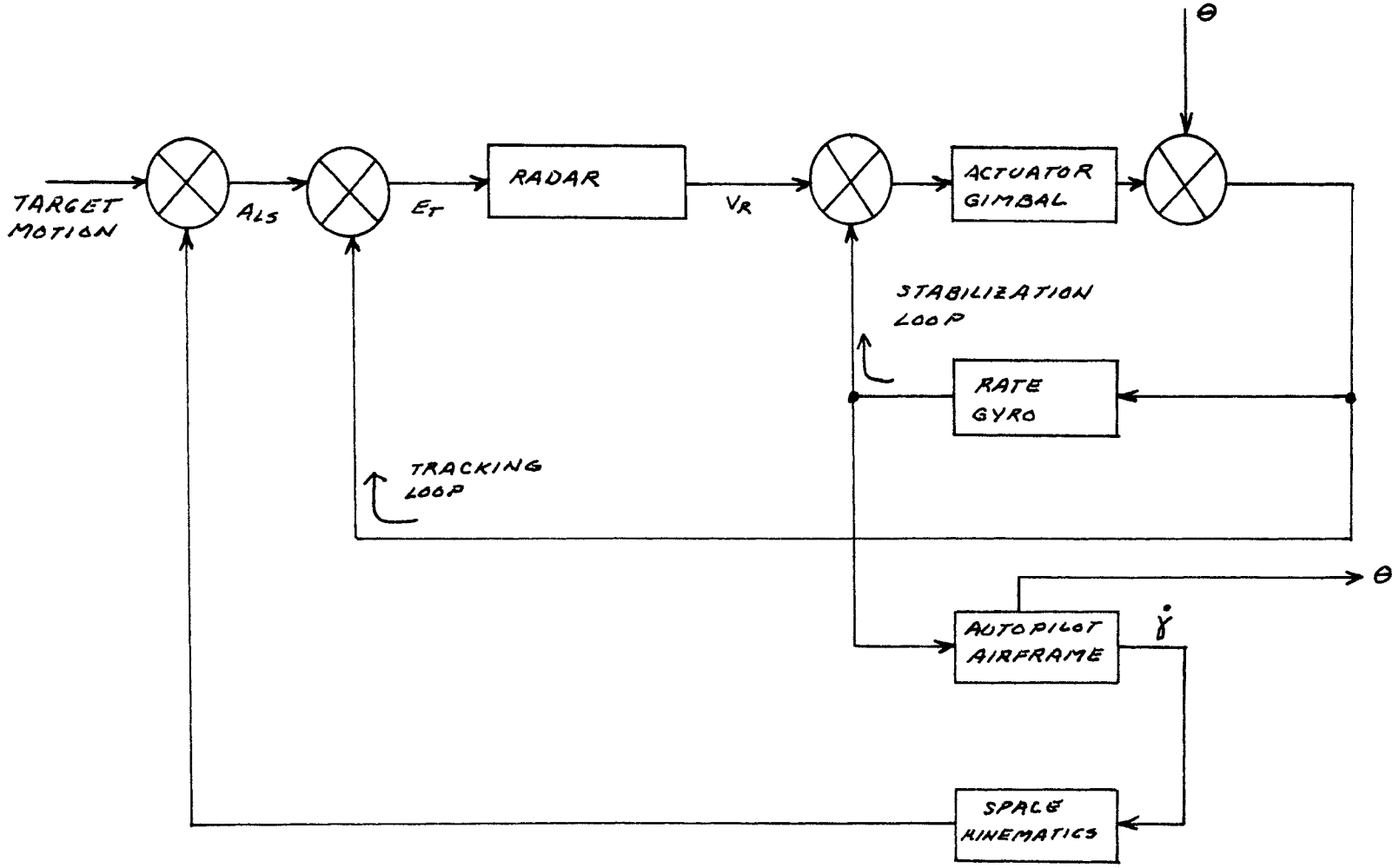

FIGURE II-2

PROPORTIONAL NAVIGATION SCHEME

TYPE I STABILIZATION LOOP

already described.

A typical Transfer characteristic of the tracking loop is:

$$G_T = G_1 G_2 / (1 + G_2 G_3)$$

Where, $G_1 = \frac{K_1 (1 + S/\omega_2)}{(1 + S/\omega_1)(1 + S/\omega_3)}$

and $\frac{G_2}{1 + G_2 G_3} = 1/K_2 S$

This gives

$$G_T = \frac{A_{TL}}{E_T} = \frac{K(1 + S/\omega_2)}{S(1 + S/\omega_1)(1 + S/\omega_3)}$$

The frequency where the amplitude of G_T is zero Db defines the open loop bandwidth, ω_C , of the tracking loop (often referred to as the crossover frequency). Typical break frequencies for this type of servo give a slope at crossover of 20 Db per decade providing stabilization of the tracking loop.

Random errors in the tracking rate $\dot{A}_{LS}$ are made up of gyro inaccuracies, radar noise transmitted through the tracking loop to the gyro output, and antenna rates caused by the platform motion which is attenuated by the stabilization loop. Bias errors are contributed by the servo steady-state and transient errors and are a function of the servo type and servo bandwidth.

A small discussion is included on the error sources to add continuity to the discussion, however, the majority of this article is occupied by the treatment of the glint problem. In addition, the error dependence will be shown. This is done since for the majority of situations, the bandwidth of the system is the means by which the servo engineer accomplishes the compromise between system dynamic response and noise sensitivities.

Figure II-4 contains a table listing the principal error sources in addition to glint which is considered for this analysis to be the major component of radar noise at short range. The expressions for the errors are developed as a supplement to the table. For this radar seeker model, gyro bias error is considered negligible.

To evaluate the error coefficients, one expands $\frac{1}{1+G(s)}$ into a Maclaurin series into the form,

$$\frac{1}{1+G(s)} = \frac{1}{1+K_P} + \frac{1}{K_V}s + \frac{1}{K_A}s^2 + \text{-----}$$

These coefficients have been evaluated and are listed in reference 3 and the values are:

$$K_V = K$$

$$K_A = \frac{K}{K(1/\omega_1 + 1/\omega_3 - 1/\omega_2) - 1}$$

Some simplification can be made if the following assumptions are valid,

$$\omega_1/\omega_2 << 1, \quad \omega_3 >> \omega_1, \omega_2$$

$$G_T \cong \frac{K\omega_1(s/\omega_2+1)}{s^2}$$

and for this function

$$K_A = \frac{\omega_c^2}{\omega_c/\omega_2} = \omega_c\omega_2$$

and, $K_V = K_A/\omega_1 = \omega_c(\omega_2/\omega_1)$

C. Derivation of Error Sources

Stabilization - The following figure represents the seeker simplified block diagram redrawn for a disturbance input θ.

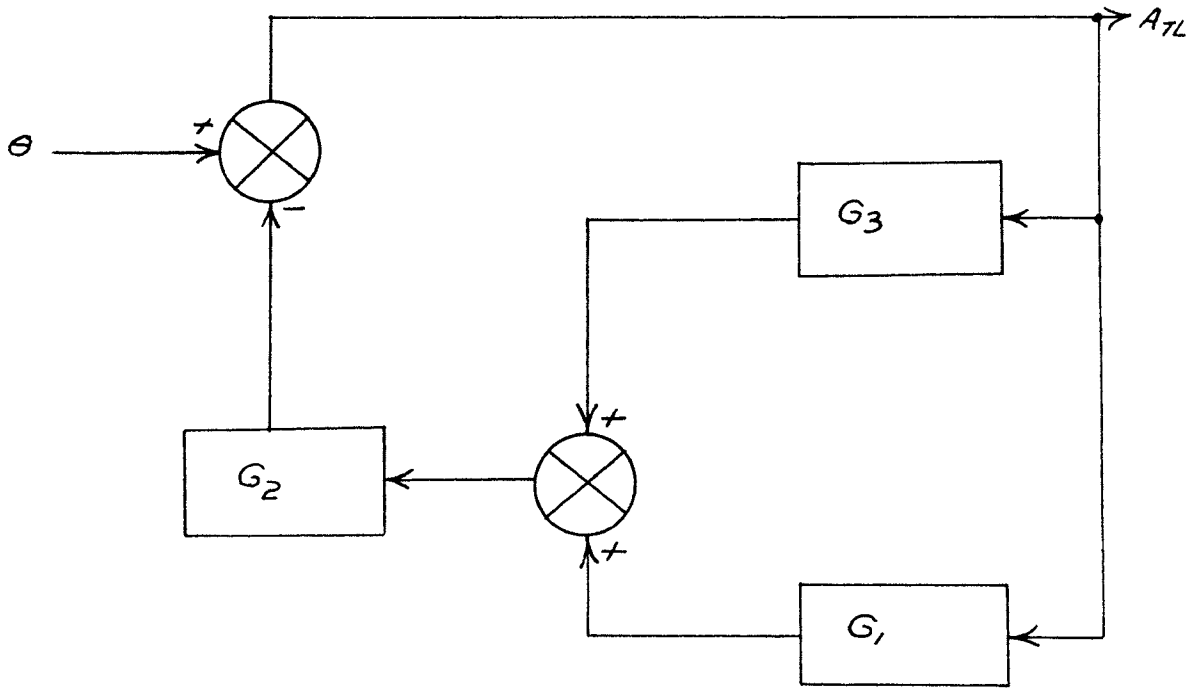

FIGURE II-3

Simplified Block Diagram for a Disturbance Input θ

The transfer function from output to input is:

$$\frac{A_{TL}}{\theta} = \frac{1}{1+G_2(G_1+G_3)} \cong \frac{1}{G_2 G_3}$$

The output rate error for a disturbance rate $\dot{\theta}$ is:

$$\dot{A}_{TL} = \frac{\dot{\theta}}{G_2 G_3}$$

This results by again reducing the block diagram and solving for $\dot{A}_{TL}$ as a function of the input θ

Now if $\dot{\theta}$ is a pure sine wave of amplitude $\dot{\theta}_o$, the rms error in A_{TL} is:

$$A_{TL} = \frac{0.707\dot{\theta}_o}{|G_2 G_3|}$$

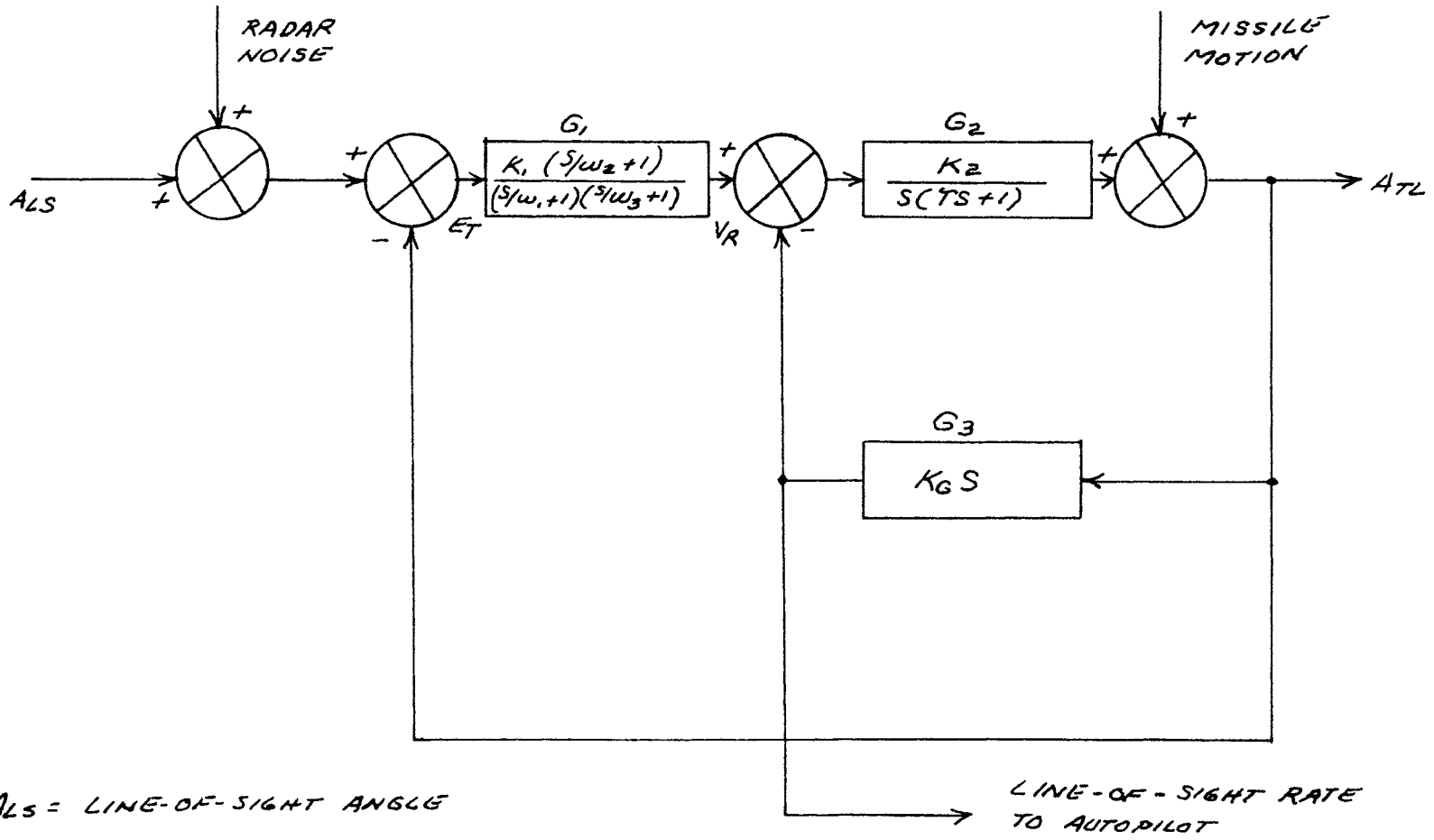

A_{LS} = LINE-OF-SIGHT ANGLE

A_{TL} = ANTENNA ANGLE

V_R = RATE COMMAND

G_1 = RADAR SHAPING NETWORK

G_2 = SHAPING NETWORK (POWER AMPLIFIER, ACTUATOR, ETC.)

FIGURE II-4
SEEKER SIMPLIFIED BLOCK DIAGRAM

TABLE II-1

TABLE OF LINE-OF-SIGHT RATE ERRORS

ERROR SOURCES	APPROXIMATE RELATIONSHIP	REMARKS
RANDOM		
GYRO RANDOM	$B\dot{A}_{LS}$	$0.002 \angle B \angle 0.02$
ANTENNA MOTION	$\frac{0.707\dot{\theta}_o}{G_2 G_3}$	Single Frequency Input Rate. Peak Amplitude
BIAS		
TRACK LOOP	$\frac{\ddot{A}_{LS}}{K_V} \quad \frac{\dddot{A}_{LS}}{K_a}$	For $G_T = \frac{K(S/\omega_2+1)}{S(S/\omega_1+1)(S/\omega_3+1)}$

III. TARGET DESCRIPTION

A. General

In describing the target, the glint problem must be defined in terms of the target size and the beamwidth of the antenna to determine the range at which the glint noise spectrum becomes significant. Two methods are used to determine the effects of target glint on terminal tracking behavior. The first is an analytic approach fashioned after the analysis of a two element target described in reference 1. The second approach is to describe the target statistically and use the results of this development as the glint noise spectrum input for the seeker. For the statistical approach, the target will be assumed to consist of a collection of individual targets whose scattering properties can be described statistically. Also, a known glint spectrum is used for comparison purposes.

Now, one would expect that the majority of these scatterers would operate in the surface and edge scattering region. The reason for this is that for good acquisition range (high antenna gains), nominal weather performance, and present state-of-the-art design capabilities most anti-ship radar seekers are presently concentrated in the region above 10 gigahertz. The smaller antenna also provides a larger target-to-clutter

discrimination although the smaller beamwidth compounds the dynamics of acquisition. This region of surface scattering is one where the optics case is being approached, therefore the geometry techniques employed in optics can be applied to obtain approximations to the scattering problem.

B. Target Optics

An analysis of an n-element target can be made, the analysis being similar to that of Locke in reference (1) page 440.

For this analysis the function for each lobe of a tracking radar antenna pattern may be expressed as a Taylor series about the crossover point as seen in Figure III-1.

$$f(\theta) = f(\theta_0) + f'(\theta-\theta_0) + \frac{1}{2!} f''(\theta-\theta_0)^2 + \cdots \qquad (3-1)$$

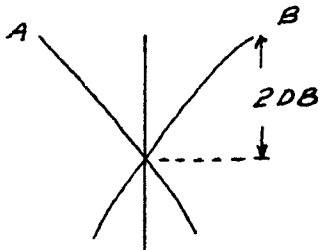

Figure III-1, Tracking Radar Lobe Pattern

For small angles off-axis, only the first two terms may be retained, which is true for an antenna response which is a linear function of the error angle, and this is the case for targets which are close to the boresight axis. Then the amplitude response can be written as,

$$e = E_o[1 \pm p(\theta - \theta_o)] \tag{3-2}$$

and for a single element target, the signal from lobe A is

$$e_A = G[1 - p(\theta_T - \theta_o)]\cos\omega t \tag{3-3}$$

and from lobe B is

$$e_B = G[1 + p(\theta_T - \theta_o)]\cos\omega t \tag{3-4}$$

where G is defined in reference [1] as lumping together target size, system gain, etc.. The detector squares e_A and e_B and a low-pass filter rejects all but the d-c term and low frequency terms and since appropriate filtering is used to filter out the second harmonic,

$$\epsilon = G^2 p(\theta_T - \theta_o)$$

and for an on-axis target, $\theta_o = \theta_T$ and $\epsilon = 0$.
Now if the target consists of two reflecting elements, each will contribute to the received signal. The returns will be at the same frequency but any phase depending upon the relative range. The nature of the problem becomes evident at this point since at relatively long ranges, where the target span is less than 5% of the radar beamwidth the target will appear to be a point source and

will continue until the radar antenna is capable of resolving the individual target elements, i.e. at relatively long ranges the return energy appears to be concentrated at a point source. Reference [1] contains the solution for two targets with the results included in graphic form. The results are included in this paper for reference purposes in the form of Figure III-2.

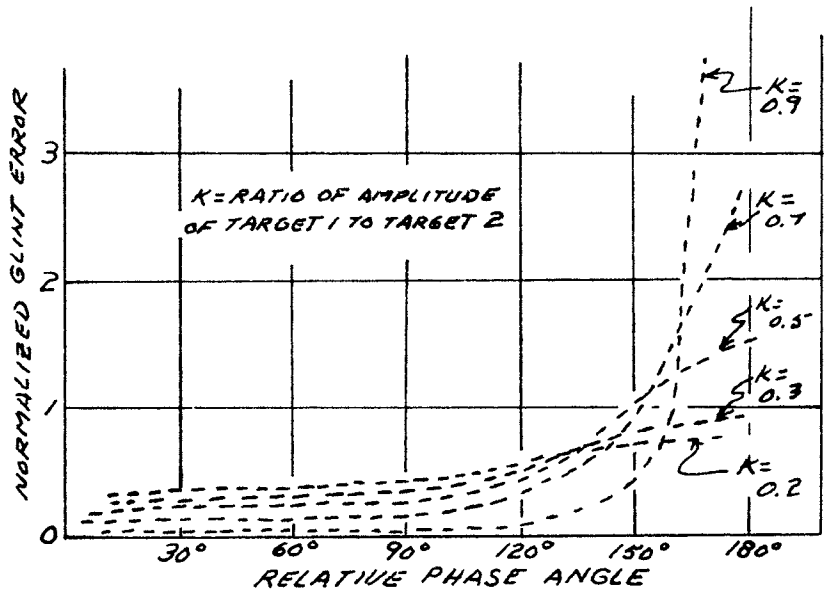

Figure III-2, Tracking Error For The Two-Element Target

Locke's result is,

$$\theta_0 = \theta_{T_1} + \theta_D \frac{a_2 + a\cos\alpha}{1 + a^2 + 2a\cos\alpha} \qquad (3\text{-}5)$$

where, α is the relative phase difference for the two target returns

θ_{T1} is the off-angle for target 1

and θ_D is the angular spacing between the target elements.

Now equation 3-5 is plotted for varying phase difference (α). Two cases are of interest, first for α = o, the two return signals are in phase. Then the coefficient of θ_D in (3-5) will reduce to $a/(a+1)$ and for 180 degrees the coefficient reduces to $a/(a-1)$ For the second case the angle of zero error will be outside the limits of the two target elements.

Now for n = 3,

$$e_B = G[1+\rho(\theta_{T_1}-\theta_0)]\cos\omega t + a_1 G[1+\rho(\theta_{T_2}-\theta_0)]\cos(\omega t+\alpha_1) + a_2 G[1+\rho(\theta_{T_3}-\theta_0)]\cos(\omega t+\alpha_3) \quad (3\text{-}6)$$

and,

$$e_A = G[1-\rho(\theta_{T_1}-\theta_0)]\cos\omega t + a_1 G[1-\rho(\theta_{T_2}-\theta_0)]\cos(\omega t+\alpha_1) + a_2 G[1-\rho(\theta_{T_3}-\theta_0)]\cos(\omega t+\alpha_2) \quad (3\text{-}7)$$

where a_1 is the amplitude ratio of target element two to target element one, and a_2 is the amplitude ratio of target element three to target element one, and α_1 and α_2 are the phase differences between target element one and target elements two and three respectively. Now to proceed with the development, e_A and e_B must be squared. The simplest approach appears to be to make the following substitutions, For e_A

$$A = G[1-\rho(\theta_{T_1}-\theta_0)] \quad (3\text{-}8)$$

$$B = a_1 G[1-\rho(\theta_{T_2}-\theta_0)] \quad (3\text{-}9)$$

$$C = a_2 G[1-\rho(\theta_{T_3}-\theta_0)] \quad (3\text{-}10)$$

Then,

$$e_A^2 = [A\cos\omega t + B\cos(\omega t+\alpha_1) + C\cos(\omega t+\alpha_2)]^2 \qquad (3\text{-}11)$$

and expanding this and using the fact that appropriate filtering will leave only the low frequency and DC term,

$$e_A^2 = A^2/2 + B^2/2 + C^2/2 + AB\cos\alpha_1 + AC\cos\alpha_2 + BC(\cos\alpha_1\cos\alpha_2 + \sin\alpha_1\sin\alpha_2) \qquad (3\text{-}12)$$

Likewise, for e_B

$$A' = G[1 + p(\theta_{T_1} - \theta_0)] \qquad (3\text{-}13)$$

$$B' = a_1 G[1 + p(\theta_{T_2} - \theta_0)] \qquad (3\text{-}14)$$

$$C' = a_2 G[1 + p(\theta_{T_3} - \theta_0)] \qquad (3\text{-}15)$$

then,

$$e_B^2 = A'^2/2 + B'^2/2 + C'^2/2 + A'B'\cos\alpha_1 + A'C'\cos\alpha_2 + B'C'(\cos\alpha_1\cos\alpha_2 + \sin\alpha_1\sin\alpha_2) \qquad (3\text{-}16)$$

substituting the corresponding values for A, B, C, A', B', and C' into the expression $\epsilon = e_B^2 - e_A^2$

$$\epsilon = 1/2[G^2 4p(\theta_{T_1} - \theta_0) + a_1^2 G^2 4p(\theta_{T_2} - \theta_0) + a_2^2 G^2 4p(\theta_{T_3} - \theta_0)] + 2\cos\alpha_1 a_1 G^2 p[(\theta_{T_1} - \theta_0) + (\theta_{T_2} - \theta_0)] + 2\cos\alpha_2 a_2 G p[(\theta_{T_3} - \theta_0) + (\theta_{T_1} - \theta_0)] + (2\cos\alpha_1\cos\alpha_2 + \sin\alpha_1\sin\alpha_2) a_1 a_2 G^2 p[(\theta_{T_2} - \theta_0) + (\theta_{T_3} - \theta_0)] \qquad (3\text{-}17)$$

For the on target conditions $\epsilon = 0$ and

$$\theta_0 = \frac{\theta_{T_1} + a_1^2\theta_{T_2} + a_2^2\theta_{T_3} + a_1\cos\alpha_1(\theta_{T_1} + \theta_{T_3}) + a_2\cos\alpha_2(\theta_{T_3} + \theta_{T_1}) + a_1 a_2(\cos\alpha_1\cos\alpha_2 + \sin\alpha_1\sin\alpha_2)}{[1 + a_1^2 + a_2^2 + 2a_1\cos\alpha_1 + 2a_2\cos\alpha_2 + 2a_1 a_2(\cos\alpha_1\cos\alpha_2 + \sin\alpha_1\sin\alpha_2)]/(\theta_{T_2} + \theta_{T_3})} \qquad (3\text{-}18)$$

Now for purposes of extracting some useful information, assume

$$\theta_{T_2} = \theta_{T_1} + \theta_D$$

and

$$\theta_{T_3} = \theta_{T_1} - \theta_D$$

Therefore,

$$\theta_o = \theta_T + \frac{\theta_D[a_1^2 - a_2^2 + a_1\cos\alpha_1 - a_2\cos\alpha_2]}{1+a_1^2+a_2^2+2a_1\cos\alpha_1+2a_2\cos\alpha_2+2a_1a_2(\cos\alpha_1\cos\alpha_2+\sin\alpha_1\sin\alpha_2)} \quad (3\text{-}19)$$

To evaluate equation (3-18) for all possible conditions would require the use of a computer and a considerable amount of programming and operating time. This does not seem justifiable when the target in reality is statistical in nature and one would penalize the seeker design by attempting to apply equation (3-18) or its successor for a model employing more target elements. However, a few cases will be investigated by using equation (3-19) in an attempt to arrive at some general considerations. For the first case, assume a_1 is equal to a_2 and the respective phase differences are zero. From equation (3-19), the indicated error is zero. For case two, assume a_1 is equal to a_2 and $\alpha_1 = 0$ and $\alpha_2 = 180^\circ$, then $\theta = \theta_T + \theta_D \frac{2a_1}{1+a_1^2}$, which indicates a fixed error. Now if $\alpha_1 = \alpha_2 = 180^\circ$, then $\theta_o = \theta_T + \theta_D(0)$, and again there is no error. The error will become infinite at those points where the denominator of (3-19) approaches zero, rearranging,

$$2a^2(1+\cos\alpha_1\cos\alpha_2+\sin\alpha_1\sin\alpha_2)+2a(\cos\alpha_1+\cos\alpha_2)+1=0$$

$$a^2+\frac{a(\cos\alpha_1+\cos\alpha_2)}{1+\cos\alpha_1\cos\alpha_2+\sin\alpha_1\sin\alpha_2}+\frac{1}{2(1+\cos\alpha_1\cos\alpha_2+\sin\alpha_1\sin\alpha_2)}=0 \quad (3\text{-}20)$$

Now this is a quadratic in a that could be programmed on a computer for solutions, if any exist. The apparent difficulty in finding a root to satisfy (3-20) might indicate that as additional target elements are added the severity of the tracking error is decreased. The solution of (3-20) and the number of roots obtained would either confirm or deny this assumption.

Figure III-3 illustrates the general missile coordinates which will be used for purposes of discussion.

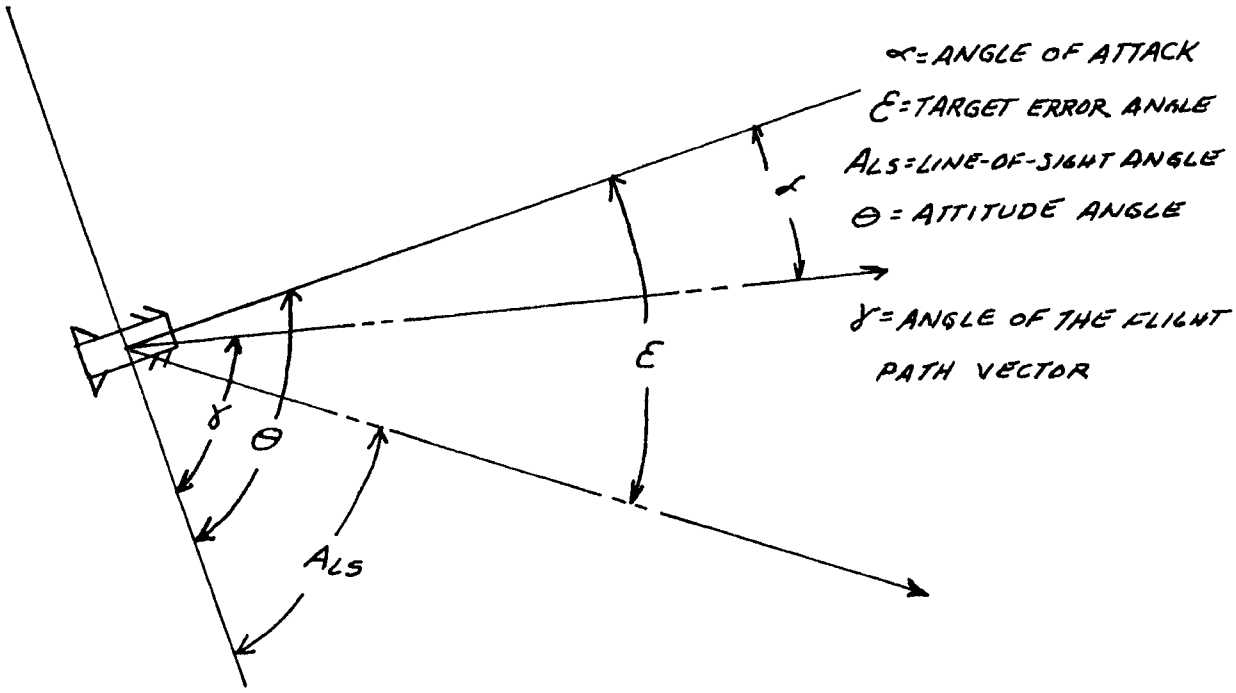

Figure III-3, General Missile Coordinates

Also, the required space geometry of the seeker and target is illustrated in Figure III-4.

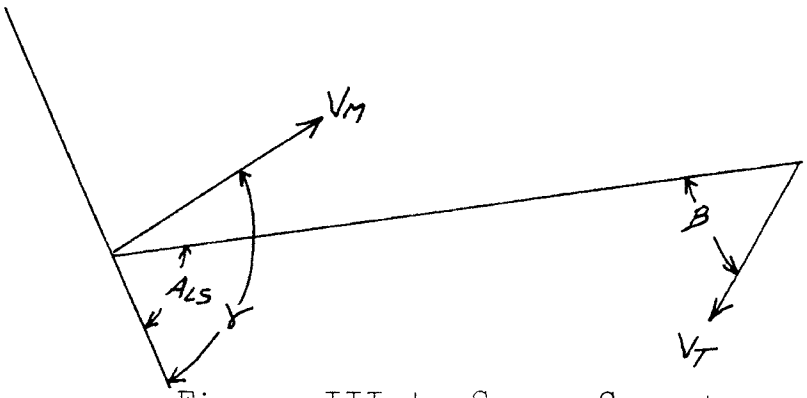

Figure III-4, Space Geometry

The angular velocity of the line-of-sight in space can be derived by finding the normal components of the missile velocity V_M and target velocity V_T with respect to the line-of-sight. From Figure III-4, the expression is,

$$-\dot{A}_{LS} = \frac{V_M \sin(\gamma - A_{LS})}{R} + \frac{V_T \sin B}{R} \qquad (3\text{-}21)$$

where,

V_M = missile velocity

V_T = target velocity

R = The range between the missile and the target

A_{LS} = Angle of line-of-sight in space

γ = Angle of the flight path vector in space

B = Angle between the target velocity vector and the missile-target line-of-sight.

Now the tracking geometry shows a dynamic environment where the relative motion of both the missile and the target provide kinematic feedback to the seeker tracking loop (see figure II-1). The error angle derived from the seeker antenna is directly related in both magnitude and sense to the error in heading of the missile.

Now for a missile airframe perturbation an error voltage is developed at the receiver output terminals which may be expressed mathematically as

$$E = K_1(\gamma - A_{LS}) \tag{3-22}$$

and, a rate of change of the angle ξ occurs which is proportional to the input displacement $\gamma - A_{LS}$. This may be expressed as

$$\dot{\xi} = \omega_1(\gamma - A_{LS}) \tag{3-23}$$

The parameter ω_1 is equal to the ratio of the missile velocity divided by the range between the missile and the target multiplied by a proportionality constant K_2. Therefore, the combined error becomes the sum of two terms. Letting K_1 equal K_2 and integrating both sides of the expression for the rate signal,

$$\frac{\xi_m}{\gamma - A_{LS}} = 1 + \omega_1/s \tag{3-24}$$

where $\omega_1 = V_M/R$

s, S = The Laplace Transform variable

$\frac{\xi_m}{\gamma - A_{LS}}$ = Assumed constant.

When the missile is at long range ω_1 is small since R is large, and ω_1 is small with respect to 1 and the effect of the integration term is small. As the range closes, the corresponding lag caused by this integration can cause instability (see reference [1], page 628).

The remaining term of equation 3-21 is considered next. In contrast to the preceding discussion the second term of the equation deals with target motion. The target motion is reflected as an error at the seeker antenna and ξ_T can be expressed as,

$$\xi_T = V_T \int_0^t \frac{\sin\beta}{R}\, dt$$

and this can be expressed as

$$\xi_{T/\beta} = \frac{V_T}{\beta} \int_0^t \frac{\sin\beta}{R}\, dt$$

If the assumption is made that during an interval of time the angle β and the range have particular values and are not functions of time, and since ξ_T may be taken to be constant $\xi_{T/\beta}$ takes the form

$$\xi_{T/\beta} = \omega_2/s \qquad (3\text{-}25)$$

where

$$\omega_2 = \frac{V_T \sin\beta}{R\beta}$$

The value of ω_2 varies with target velocity, the angles of the space geometry and the range to the target. Again at long ranges, the value of ω_2 is small so that target motion has very little to do with the rate of change of the line-of-sight angle in space. However, when the

range decreases then small perturbations in the target or missile motion may cause large variations of the target angle.

The preceding discussion illustrates that at short ranges where bandwidths are of necessity required to be larger to reduce error (Larger bandwidth here inferring shorter time constants) the rms value of the glint spectrum becomes larger, as more of this noise is introduced due to the increased bandwidth. Therefore, the next subject for discussion is the development of the glint spectrum.

C. Target Statistics

Basically radar targets behave as parasitic antennas and can be grouped into two general classes. The first class has essentially fixed geometry such as a cylinder or sphere. The second class has a geometry which is best described statistically.

The radar cross-section is a transfer function that allows us to go from the power density in the plane wave incident on the target to the power delivered per unit of solid angle in the direction of the receiving antenna. (All discussions in this article assume a far field antenna pattern, i.e. an incident plane wave at the target). The plane wave criterion is generally considered to be in effect for ranges $(R) \geq \frac{(2D)^2}{\lambda}$ where D is the diameter of the largest aperture. (A discussion is included on this subject in Appendix II). Now the scattering cross section can be analyzed using the following approach. The power collected by the receiving antenna is [The power per unit area at the target] X [The power delivered by the target per unit solid angle in the direction of the receiving antenna per unit power density at the target] X [The solid angle of the effective collecting aperature of the radar receiving antenna, as viewed from the target].

The solid angle of the receiving antenna is, by definition of solid angle, A_e/R^2 . Therefore,

$$S = \frac{P_t G_t}{4\pi R_t^2} \left[\begin{array}{l}\text{Power delivered per unit}\\ \text{solid angle in the direction}\\ \text{of the receiver per unit}\\ \text{power density at the target}\end{array}\right] \frac{A_e}{R_r^2} \qquad (3\text{-}26)$$

Now we replace the real target with one which reflects isotropically but still delivers the same power per unit solid angle in the direction of the receiving antenna (per unit power density incident at the target), then the total power that this isotropic reflector will delivery will be 4π times the middle term in equation (3-26); this power will be uniformly distributed over a sphere at any distance from the target. The fraction of this sphere occupied by the receiving antenna is $\frac{A_e}{R_r^2}\frac{1}{4\pi}$. Therefore, if we define the target's radar cross section of the isotropic reflector which delivers the same power per unit solid angle, per unit incident power density in the direction of the receiving antenna, as the actual target does the radar equation becomes

$$S = \left(\frac{P_t G_T}{4\pi R_t^2}\right)\left(\sigma\right)\left(\frac{A_e}{R_r^2}\right)\left(\frac{1}{4\pi}\right) \qquad (3\text{-}27)$$

The previous definitions can be combined to express the received energy as: the power received over the solid angle of the receiving antenna aperature is equal to [The power incident at the target per unit area] X σ X $\frac{1}{4\pi}$ [The solid angle at the receiving aperture].

Or,

$$\sigma = 4\pi \left\{ \frac{\text{Power delivered per unit solid angle in the direction of the receiver}}{\text{power per unit area incident at the target}} \right\} \quad (3\text{-}28)$$

The power delivered to the surface area of a unit solid angle, at the receiver, is $P_r R_r^2$ where P_r is the power per unit area in the plane wave, at a distance R_r from the scatterer (i.e. at the receiving antenna). If P_i is the power per unit area incident at the scatterer, then,

$$\sigma = \frac{4\pi P_r R_r}{P_i} \quad (3\text{-}29)$$

Now the average power density of a plane wave is

$$P = \frac{1}{2} |\bar{E}||\bar{H}| = \frac{1}{2} \frac{|\bar{E}|^2}{\eta} = \frac{1}{2} \eta |\bar{H}|^2 \quad (3\text{-}30)$$

where $\bar{E}$ = Electric Field Strength

$\bar{H}$ = Magnetic Field Intensity

η = The intrinsic impedance of the propogating medium combining equations 3-29 and 3-30,

$$\sigma = 4\pi R_r^2 \frac{|\bar{H}_r|^2}{|\bar{H}_i|^2} = 4\pi R_r^2 \frac{|\bar{E}_r|^2}{|\bar{E}_i|^2} \quad (3\text{-}31)$$

and a far field definition of equation 3-31 is,

$$\sigma = 4\pi \lim_{R_r \to \infty} R_r^2 \frac{|\bar{H}_r|^2}{|\bar{H}_i|^2} = 4\pi \lim_{R_r \to \infty} R_r^2 \frac{|\bar{E}_r|^2}{|\bar{E}_i|^2} \quad (3\text{-}32)$$

This last expression is the one invariably used to determine the radar cross section after the scattering problem for the reflected field strength has been solved.

Now for large targets, where local surface currents in one part are relatively independent of the current in another part, the reflected field at the receiving antenna is the vector sum of the fields which have arisen from each component target separately. If $\bar{E}_{rk}$ is the reflected field produced by the k^{th} element and d_k is the distance of this element from the receiver then,

$$|\bar{E}_r| = \left| \sum_{k=1}^{n} |\bar{E}_{rk}| e^{j(4\pi d_k/\lambda)} \right| \qquad (3\text{-}33)$$

Because, even at closing ranges, the parts of the target are relatively close together compared to the distance between the transmitter and the target, the incident field strength $\bar{E}_i$ is approximately the same on all the parts of the target, therefore,

$$\frac{|\bar{E}_r|}{|\bar{E}_i|} = \left| \sum_{k=1}^{n} \frac{|\bar{E}_{rk}|}{|\bar{E}_{ik}|} e^{j\,4\pi d_k/\lambda} \right| \qquad (3\text{-}34)$$

and substituting this result in equation (3-32)

$$\sigma = \left| \sum_{k=1}^{n} \sqrt{\sigma_k}\, e^{j(4\pi d_k/\lambda)} \right|^2 \qquad (3\text{-}35)$$

This equation will form the basis for constructing a statistical target model. An example for a two element target is,

$$\begin{aligned} \sigma &= \left| \sum_{k=1}^{2} \sqrt{\sigma_k}\, e^{j(4\pi d_k/\lambda)} \right|^2 \\ &= \left| \sqrt{\sigma_1}\, e^{j\,4\pi d_1/\lambda} + \sqrt{\sigma_2}\, e^{j\,4\pi d_2/\lambda} \right|^2 \\ &= \sigma_1 + \sigma_2 + 2\sqrt{\sigma_1 \sigma_2} \cos\left[\frac{4\pi}{\lambda}(d_1 + d_2)\right] \end{aligned}$$

Now using the previously developed equation, the basic assumption required to justify the use of this

expression is that the total field produced by a group of individual scatters is a linear combination of the fields that would arise from each individual element if the elements acted by themselves. Therefore, the elements act as independent scatters, and there is no mutual coupling. In addition, the assumption is made that the individual cross sections remain constant.

The time during which the glint spectrum applies is short, therefore, the phase $\frac{4\pi d_k}{\lambda}$ is a random variable which can take on any value from zero to 2π . The desired cross section, from equation 3-35 is the vector sum of n vectors which have random relative phase. Assuming that all of the scattering elements are identical (all of the σ_k's are equal) and calling the value of the cross section of any one element σ_o , equation 3-35 becomes

$$\sigma = \left| \sum_{k=1}^{n} \sqrt{\sigma_o}\, e^{j \frac{4\pi d_k}{\lambda}} \right|^2 \qquad (3\text{-}36)$$

Statistically this problem is identical to the isotropic two-dimensional random walk where n successive steps of fixed length σ_o are taken and where the direction of each step is completely random. If we consider the x-component of the k^{th} step to be $\sqrt{\sigma_o} \cos \frac{4\pi d_k}{\lambda}$ and the y-component of the k^{th} step to be $\sqrt{\sigma_o} \sin \frac{4\pi d_k}{\lambda}$, then the joint probability density function of components (x, y) after n steps is,

This result can be justified as follows, for two sets $\{K_S(t)\}$ and $\{K_n(t)\}$ which are independent, the joint probability density function is,

$$p(s,n) = P_1(s) P_2(n) \tag{3-45}$$

Now let,

$y = s + n$ in order to define y for a particular s, then

$$n = y - s \tag{3-46}$$

therefore for each s the integrand for the convolution integral becomes

$$P_1(s) P_2(y-s) \tag{3-47}$$

Now s can take any value from $-\infty$ to ∞, therefore summing over all possible s gives the result. Now let $Y_1(j\omega)$ and $Y_2(j\omega)$ be the Fourier Transform of $P_1(s)$ and $P_2(s)$ respectively, and these are defined by,

$$Y_1(j\omega) = \int_{-\infty}^{\infty} e^{-j\omega s} P_1(s)\, ds \tag{3-48}$$

$$Y_2(j\omega) = \int_{-\infty}^{\infty} e^{-j\omega n} P_2(n)\, dn \tag{3-49}$$

Now from equation (III-47),

$$p(y) = \int_{-\infty}^{\infty} P_1(s) P_2(y-s)\, ds$$

and

$$Y(j\omega) = \int_{-\infty}^{\infty} e^{-j\omega y} p(y)\, dy$$

therefore,

$$Y(j\omega) = \int_{-\infty}^{\infty} e^{-j\omega(s+n)} \int_{-\infty}^{\infty} P_1(s) P_2(y-s)\, ds\, dy \tag{3-50}$$

Equation III-53 can be expanded to show

$$Y(j\omega) = Y_1(j\omega) Y_2(j\omega) \tag{3-51}$$

Then, the probability density function $p(y)$ is given by taking the inverse transform of equation (3-51)

or,

$$p(y) = \frac{1}{2\pi} \int_{-\infty}^{\infty} e^{jwy} Y_1(jw) Y_2(jw)\, dw \qquad (3\text{-}52)$$

This last expression illustrates that the probability density function for the sum of independent random variables may be obtained by first determining the Fourier Transforms of the individual distributions and then by calculating the inverse Fourier Transform of their products.

To illustrate the modified spectrum due to additional target elements the individual target statistical characteristics will be assumed to be normal. Suppose that $P_1(s)$ and $P_2(n)$ are governed by independent normal distribution such that

$$P_1(s) = \frac{1}{\sigma_1 \sqrt{2\pi}} e^{-(s-m_1)^2/2\sigma_1^2} \qquad (3\text{-}53)$$

and

$$P_2(n) = \frac{1}{\sigma_2 \sqrt{2\pi}} e^{-(n-m_2)^2/2\sigma_2^2} \qquad (3\text{-}54)$$

Now to obtain $p(y)$ the Fourier Transforms of $P_1(s)$ and $P_2(n)$ must be obtained.

The resulting inverse transform is

$$p(y) = \frac{1}{\sigma \sqrt{2\pi}} e^{-(y-m)^2/2\sigma^2} \qquad (3\text{-}55)$$

where

$$m = m_1 + m_2 \qquad (3\text{-}56)$$

and

$$\sigma^2 = \sigma_1^2 + \sigma_2^2 \qquad (3\text{-}57)$$

Thus the sum of two independent normals is also a normal distribution* with the resulting mean and the variance equal to the sum of the individual means and variances. This analysis can be applied to the sum of many independent variables. These results are illustrated in figure III-6.

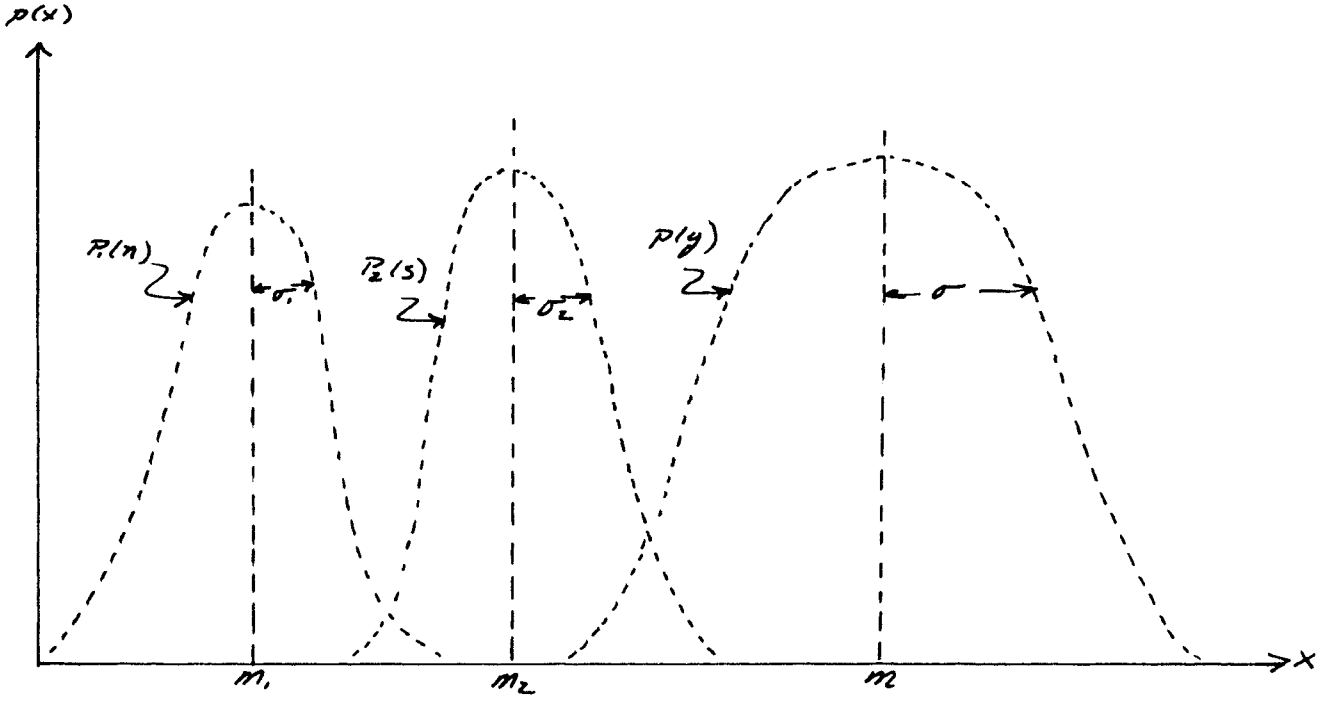

Figure III-6,
Probability Density Function for Sum of Two Normal Distributed Variables

Therefore, the standard deviation of the total glint is a function of the target size

---

*These are classical results, C.F. Reference (1) p. 390.

IV. GLINT MODEL EVALUATION

A. General

The previously defined model will now be used to evaluate the effect of glint on the angle tracking performance of this seeker.

B. Seeker Performance as a Function of Glint

The average angle of arrival, $\sigma_L = \sqrt{\Phi(0)}$ about the actual direction of the main target is (see reference [3]) for a two-element target.

$$\sigma_L = \left(\frac{L \cos\phi}{R}\right) K' \cos\varphi \quad * \tag{4-1}$$

where

$$\phi = 2L\pi \sin\varphi/\lambda \tag{4-2}$$

ϕ = angle between the target axis and radar wave front

R = range to target

K = ratio of signal amplitude from major and minor reflectors.

The mean square value of the rate error due to glint is given by

$$(\dot{\sigma}_0)^2 = \frac{1}{2\pi j}\int_{-j\infty}^{j\infty} \left| \frac{S\,G_T(s)}{1+G_T(s)} \right|^2 \Phi(s)\,ds \tag{4-3}$$

where $\frac{G_T}{1+G_T}$ is the tracking loop transfer function previously defined and s represents the differentiation performed by the gyro.

---

*See Appendix III.

For large ω_3 and for $\omega_1/\omega_2 \ll 1$

$$\frac{G_T}{1+G_T} = \frac{K_a\,(s/\omega_2+1)}{s^2+K_a(s/\omega_2+1)} \qquad (4\text{-}4)$$

where,

$$G_T \cong K_a\,(s/\omega_2+1)/s^2 \qquad (4\text{-}5)$$

Now substituting into the previous expression for the mean square value of rate error, (see reference 11, page 458)

$$(\dot{\sigma}_o)^2 = \frac{1}{2\pi j}\int_{-j\infty}^{j\infty} \frac{s\,K_a(s/\omega_2+1)}{s^2+K_a(s/\omega_2+1)} \frac{\sigma_i^2\,\omega_g^2}{\omega_g^2-s^2}\,ds \qquad (4\text{-}6)$$

Now putting this expression into a form given in a table of integrals (reference 8, page 369),

$$(\dot{\sigma}_o)^2 = K_a^2\sigma_i^2\omega_g^2\left[\frac{1}{2\pi j}\right]\int_{-j\infty}^{j\infty} \frac{s^4/\omega_3^2 - s^2}{\left[s^3+(\omega_g+\frac{K_a}{\omega_2})s^2+(K_a+\frac{K_a\omega_g}{\omega_2})s+\omega_g K_a\right][h(-s)]} \qquad (4\text{-}7)$$

The solution for the integral given in the table is

$$I = \frac{-K_a(1+\omega_2/\omega_a)}{2[\omega_g K_a-(\omega_g+\frac{K_a}{\omega_2})(K_a)(1+\frac{\omega_g}{\omega_2})]\omega_a^2} - 1 \qquad (4\text{-}8)$$

therefore

$$(\dot{\sigma}_o)^2 = K_a^2\sigma_i^2\omega_g^2\left\{\frac{K_a(1+\omega_g/\omega_2)+\omega_2^2}{2K_a[(\omega_g+\frac{K_a}{\omega_2})(1+\frac{\omega_g}{\omega_a})-\omega_g]\omega_2^2}\right\} \qquad (4\text{-}9)$$

substituting into the above expression

$$K_a = \omega_0^2/\sqrt{1+K^2} \cong \omega_c^2/K$$

$$K = \omega_c/\omega_a$$

$$r = \omega_c/\omega_g$$

where ω_c is the crossover frequency of $G_T(s)$

$$\frac{\dot{\sigma}_o}{\omega_c\sigma_i} = \left[\left(\frac{\omega_2}{2K}\right)\left(\frac{K^2+Kr+r}{K+Kr+r^2}\right)\right]^{1/2}$$

Sample calculation of seeker rate error

Glint-Assumed values for target and kinematics values are as follows:

$K' = 0.1$

$L = 10$ (meters)

$R = 300$ (meters)

$\psi = 0$

$\omega_a = 0.001, 0.01,$ and 0.02 rad/sec

Substituting into the expression for the average glint angle,

$$\sigma_i = L \cos\phi K' \cos\phi$$

$$= 0.0033 \text{ rad.}$$

using a Ku-Band radar where the wavelength is assumed to be 1.84cm and the glint noise bandwidth is

$$\omega_g = 2$$

$$= 6830\,\omega_a$$

$$= 6.83, 68.3, \text{ and } 136.6 \text{ rad/sec}$$

For the above computed values of σ_i and ω_g, σ_o is plotted as a function of the open tracking loop bandwidth, ω_c in Figure (IV-1). From the curves of figure (IV-1) for ω_c equal to 6.28 rad/sec.

GLINT PRODUCED RATE ERROR AS A FUNCTION OF

TRACKING LOOP BANDWIDTH

FIGURE IV-1

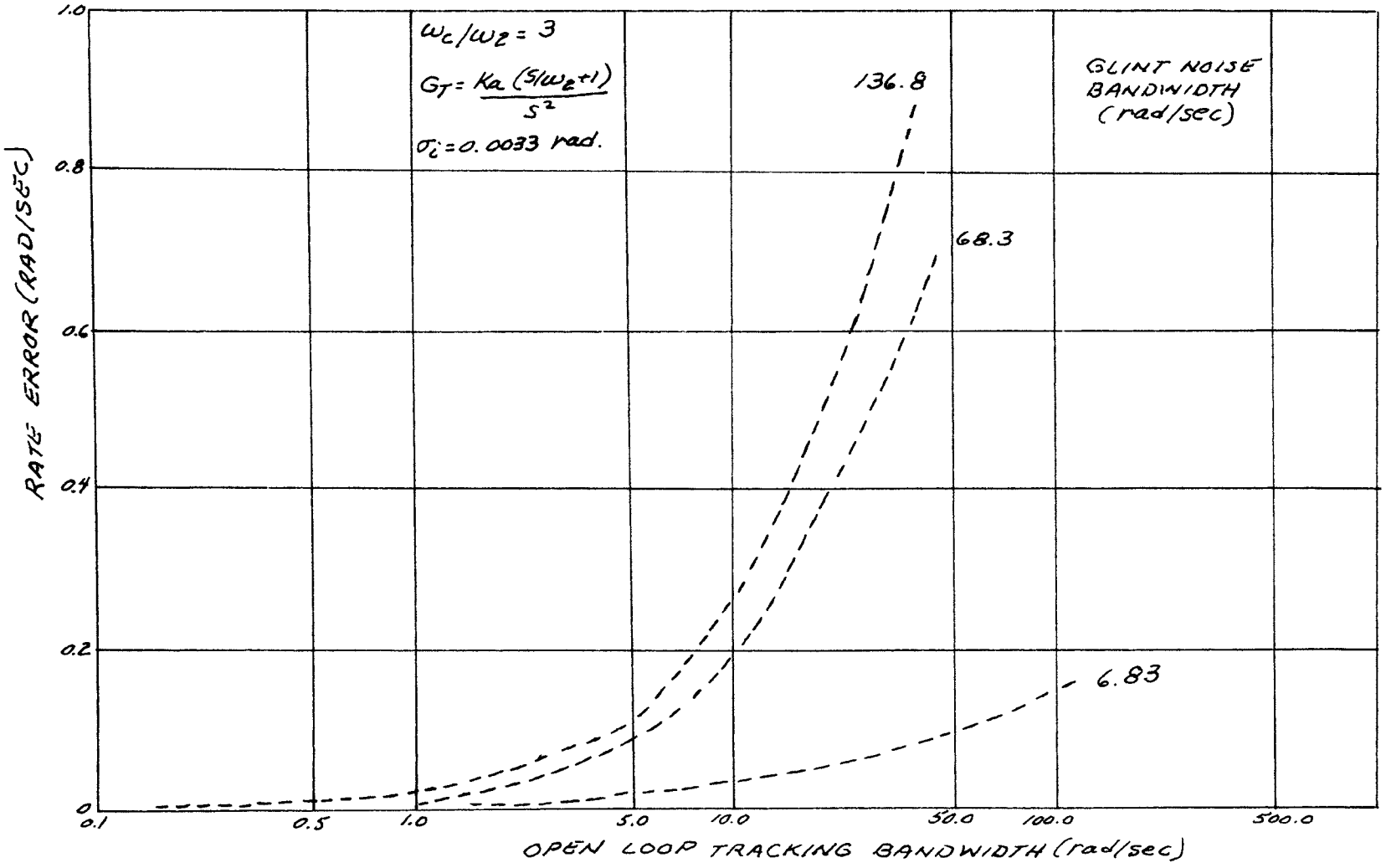

GLINT BANDWIDTH (rad/sec)	RATE ERROR (rad/sec)
6.83	0.03
68.3	0.12
136.6	0.16

V. A RECENT GLINT REDUCTION TECHNIQUE

A. General

Recent technological advancements have provided means for reducing radar tracking errors by utilizing a principle commonly called frequency agility. The effect of glint on the accuracy of radar angle tracking has been described in the previous sections of this report. This section is devoted to describing analytically, the improvement which can be derived by using a frequency agile technique.

B. Analytic Improvement Factor

For the purposes of this section, whether or nct glint is a significant problem with a fixed frequency radar is not considered.

Analysis - The reduction in glint tracking angle noise afforded by frequency agile radar can be derived on a very much simplified basis. The basic reason for the improvement is that the frequency agile radar obtains more independent samples in a given time than does the fixed frequency radar.

If the frequency agile radar jumps rapidly and far enough so that each pulse is completely uncorrelated, the number of independent samples per second is simply equal to the pulse repetition rate, f_r.

$$N_1(FA) = f_r \tag{5-1}$$

If the frequency agile radar does not have unlimited bandwidth, then the number of independent samples per second is equal to the number of independent frequency samples that can be obtained in one second. This is dependent on the total frequency agile bandwidth, the correlation bandwidth of the target, Δf , and the correlation time of the glint, t_g . The correlation bandwidth of the target is given as

$$\Delta f = \frac{C}{2D} \tag{5-2}$$

where C is the velocity of light, and D is the length of the target in the range direction. For example, a target 15 meters long will have a correlation bandwidth of 10 MHz. When the number of independent samples is bandwidth limited, the number of independent samples per second is then

$$N_2(FA) = \left(\frac{B}{\Delta f}\right)\left(\frac{1}{t_g}\right) \tag{5-3}$$

In a typical case, B equals 500 MHz, $\Delta f = 10\,MHz$, and t_g = 0.05 sec. For this case,

$$N_2(FA) = \left(\frac{500}{10}\right)\left(\frac{1}{0.05}\right) = 1000 \qquad (5\text{-}4)$$

Since we have generally been considering PRF's of over 1,000, we will find that the number of independent samples is bandwidth limited rather than PRF limited.

The total number of possible independent samples per second is 1,000; but if we use a random tuning system, we will have some repetition, and thus some fraction of the 1,000 will be identical pieces of information, not independent samples. We will later show that the average fraction of independent samples is about 70% to 90% of the maximum possible. Assuming a value of 80% for the case described ($\bar{M} = 0.$), we obtain 800 independent samples per second.

Now for a fixed frequency radar, the number of independent samples per second is simply the reciprocal of the glint correlation time.

$$N_{FF} = \frac{1}{t_g} \quad \text{per second} \qquad (5\text{-}5)$$

The ratio of the improvement of the frequency agile radar to the improvement of the fixed frequency is,

$$I = \sqrt{\frac{N_{FA}}{N_{FF}}} = \sqrt{\frac{\bar{M}B}{\Delta f} \cdot \frac{t_g}{t_g}} = \sqrt{\frac{\bar{M}B}{\Delta f}} \qquad (5\text{-}6)$$

As an example, with an agility bandwidth of 500 MHz, a glint correlation bandwidth of 10 MHz, and $\bar{M} = 0.8$

$$I = \sqrt{0.8\left(\frac{500}{10}\right)} = \sqrt{42}$$
$$= 6.5$$

Barton, Reference [3], gives the effective number of pulses integrated as $\frac{f_r}{2B_n}$ where B_n is the servo bandwidth. The reduction in glint is proportional to the square root of the number of pulses integrated; thus the improvement factor is

$$I_1(FA) = \sqrt{\frac{f_r}{2B_n}} \quad \text{(PRF Limited)} \qquad (5\text{-}7)$$

or

$$I_2(FA) = \sqrt{\frac{B}{\Delta f}\frac{1}{t_g}\frac{1}{2B_n}\bar{M}} \quad \text{(Bandwidth Limited)} \qquad (5\text{-}8)$$

whichever is smaller.

For fixed frequency,

$$I(FF) = \sqrt{\frac{1}{t_g}\frac{1}{2B_N}} \qquad (5\text{-}9)$$

Note that for both fixed frequency and frequency agile radars, the tracking error is reduced by decreasing the tracking servo bandwidth.

To calculate the fraction of the pulses which are independent, we will assume that the bandwidth, B, is broken up into n discrete frequency resolution cells.

$$n = \frac{B}{\Delta f}, \text{ each } \Delta f \text{ wide} \qquad (5\text{-}10)$$

We now generate a group of z samples (some are independent, some may not be). If we plot a typical histogram, it will look something like Figure V-1.

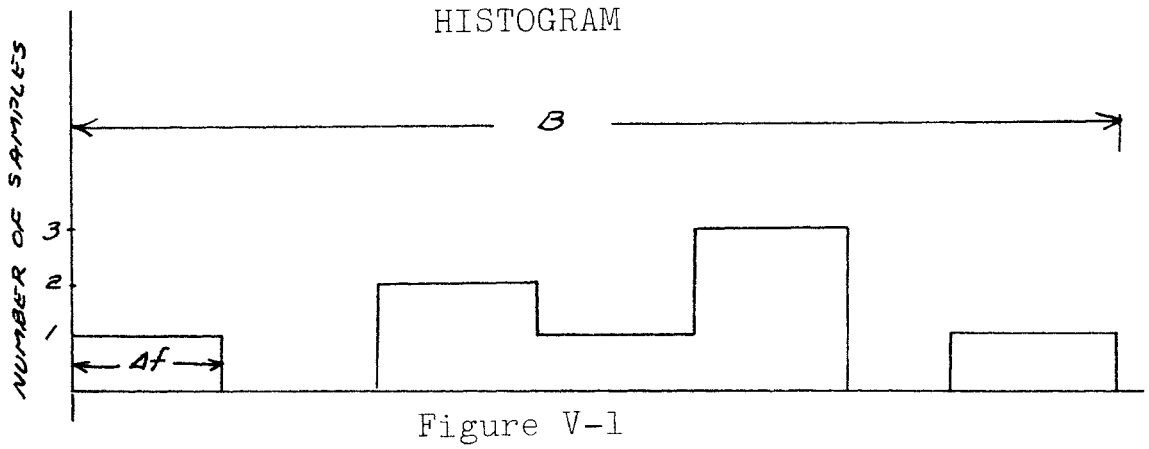

Figure V-1

The probability of getting a hit on one trial is $\frac{1}{n}$. The probability of getting a zero in any one resolution cell on all z trials (samples) is

$$P_0 = \left(1 - \frac{1}{n}\right)^z \tag{5-11}$$

The number of samples is simply the number of pulses in one glint correlation time period: z equals $PRF \cdot t_g$

We will now set out to compute the average number of empty cells. Let K be the number of empty cells. Then the average number of empty cells, $\bar{K}$, is:

$$\bar{K} = \sum_{K=0}^{n} K P_K \tag{5-12}$$

$P(K=0)$ = probability of $K=0$ (all have at least one), or the probability of any one cell not empty = $1-P_0$

$P(K=0)$ = probability of all cells not empty = $(1-P_0)^n$

$P(K=1)$ = probability of $K=1$

$P(K=1)$ = probability of one cell empty and all others not empty. The probability of a specific cell being empty and the rest not empty is

$$P(1) = P_0(1-P_0)^{n-1}$$

Now there are $\binom{n}{1}$ ways of choosing which one is empty; therefore,

$$P(K=1) = \binom{n}{1} P_0 (1-P_0)^{n-1}$$

and

$$P(K=2) = \binom{n}{2} P_0^2 (1-P_0)^{n-2}$$

The general term is obviously

$$P(x) = \binom{n}{x} (P_0)^K (1-P_0)^{n-K}$$

This is the binomial distribution. (We could have possibly arrived at this conclusion by inspection of the process.) The average number of empty cells (R) is then

$$\bar{K} = nP_0 = n\left(1-\frac{1}{n}\right)^2$$

$$\bar{M} = \frac{n-\bar{K}}{n} = 1-\frac{\bar{K}}{n} = 1-\left(1-\frac{1}{n}\right)^2$$

Substituting $\bar{M}$ back into equation (6) for the improvement over a fixed frequency radar, we get:

$$I = \sqrt{\left(1-\left[1-1/n\right]^2\right)\frac{B}{\Delta f}} \qquad (5\text{-}13)$$

$$I = \sqrt{\left(1-\left[1-\frac{\Delta f}{B}\right]^{\text{PREF. by}}\right)\frac{B}{\Delta f}} \qquad (5\text{-}14)$$

and substituting for Δf

$$I = \sqrt{\left[1-\left(1-\frac{c}{2DB}\right)^{PRF.t_g}\right]\frac{2DB}{c}} \qquad (5\text{-}15)$$

putting in the value of c

$$I = \sqrt{\left[1-\left(1-\frac{3\times10^8}{2DB}\right)^{PRF.t_g}\right]\frac{2DB}{3\times10^8}} \qquad (5\text{-}16)$$

$$= \sqrt{\left[1-\left(1-\frac{3\times10^8}{2B}\right)^{\infty}\frac{2B}{3\times10^8}\right]} \quad \left\{\begin{array}{l}\text{where } PRF.t_g=\infty \\ DB=B\end{array}\right. \qquad (5\text{-}17)$$

$$= \sqrt{\left[1-\left(1-\frac{1.5\times10^8}{B}\right)^{\infty}\right]\frac{B}{1.5\times10^8}} \qquad (5\text{-}18)$$

Results - The improvement factor is plotted in Figure (V-2) as a function of the ratio PRF to glint bandwidth. Note that increasing the agility bandwidth is the most significant factor influencing the improvement factor. Note that this improvement is with respect to a fixed frequency radar. Both types can effect a further glint reduction by averaging the glint over a time period long compared to the glint correlation time (for example, by the tracking servo bandwidth). Since this factor affects both radar types equally, it wasn't analyzed here.

Analytical Approximations - Some approximations were used in this analysis, and hence the results can only be viewed as approximations. For example, equation (5-15) gives the number of independent samples per second as the reciprocal of the glint correlation time. This would only be strictly true if the glint

FREQUENCY AGILITY GLINT IMPROVEMENT

FIGURE V-2

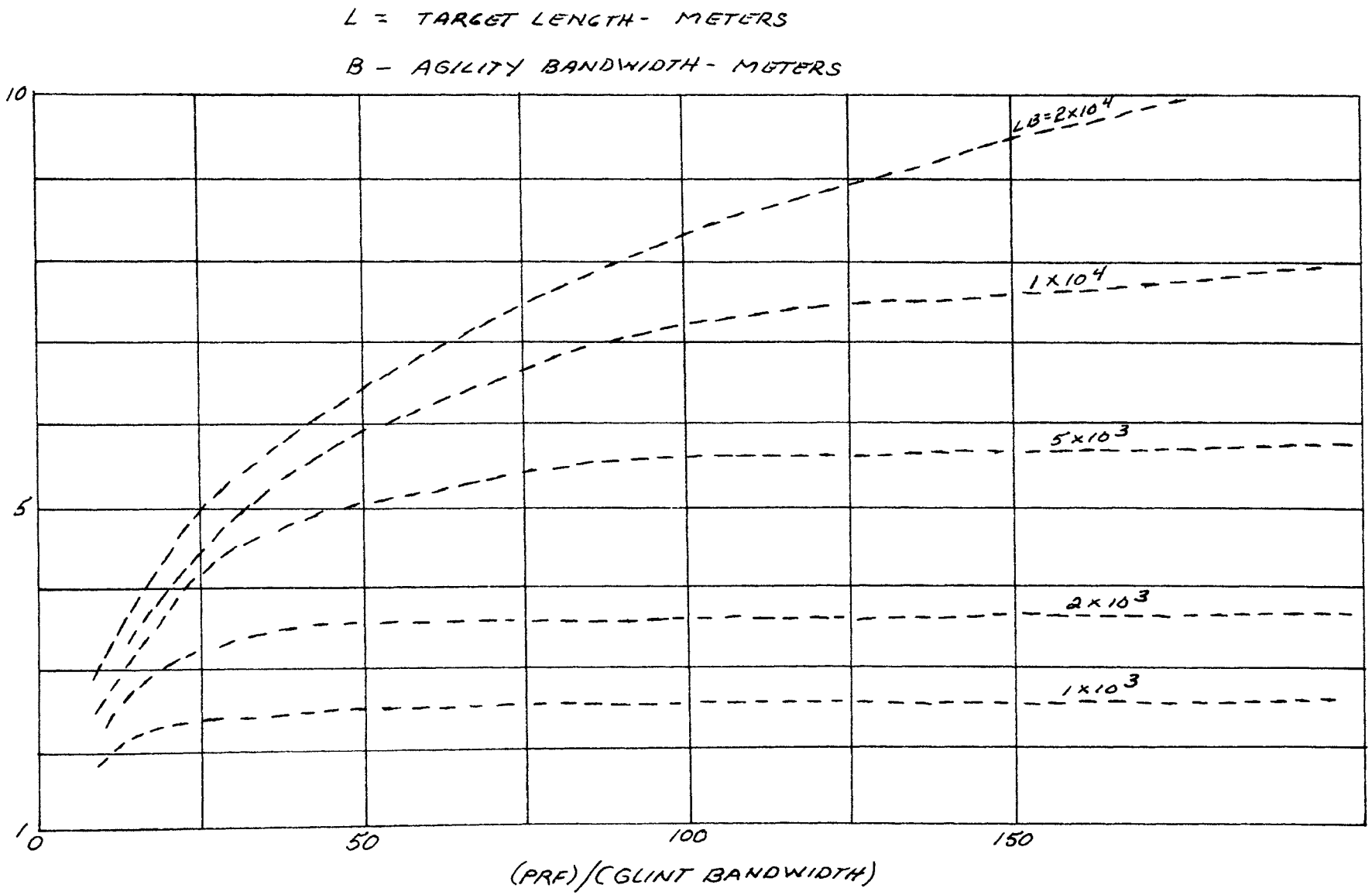

autocorrelation function were unit from zero to t_g, and zero elsewhere, which is a physical impossibility. This approximation is shown below.

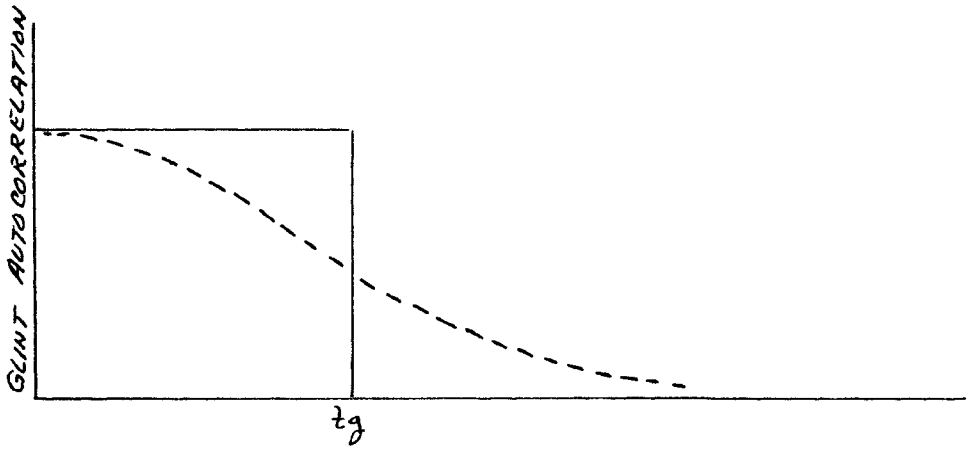

FIGURE V-3

GLINT AUTOCORRELATION APPROXIMATION

A further approximation is that $t_g = \frac{1}{B_g}$. For a description of this approximation, see Reference [10], pages 435 and 436. It is felt that the total uncertainty introduced by these approximations should be less than a factor of about 1.5.

VI. CONCLUSIONS

An analytical approach was used to describe the effect of Glint (angle noise) on the dynamic tracking characteristics of a missile seeker. The equations which resulted were too cumbersome for extracting useful information without the aid of a computer for a target model with more than two reflecting elements. This approach does not adequately describe the physical target because the return energy actually has a statistical distribution for all but the very simple geometric bodies.

The statistical approach fashioned after the classical random walk problem (from statistics) was used to develop a statistical distribution. The resulting distribution was Rayleigh and transforming this into spectral form illustrated that a low frequency distribution resulted which is similar to present day glint models derived from experimental data. The results were then incorporated into the classical statistical analysis of feedback control systems with the conclusion that glint is the predominant error source for closing ranges.

In addition, a new technique was discussed and analysis showed that an improvement can be obtained by reducing the effect of glint through the use of frequency agile techniques.

VII. APPENDICES

A-PROPORTIONAL NAVIGATION*

1. Definition: A proportional-navigation course is a course in which the rate of change of missile heading is directly proportional to the rate of rotation of the line-of-sight from the missile to the target.

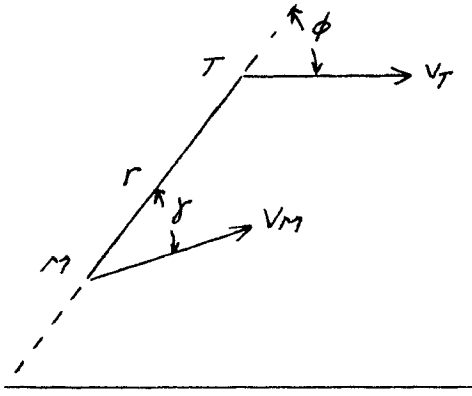

r = instantaneous missile-to-target range
M = missile position
V_T = target velocity
V_M = missile velocity
ϕ = angle between target velocity vector and line-of-sight
ϕ_M = missile heading
γ = missile heading relative to line-of-sight
T = target position

Figure AI-1, Proportional-Navigation Geometry

As an aid to deriving the radial and transverse components Figure AI-2 can be used,

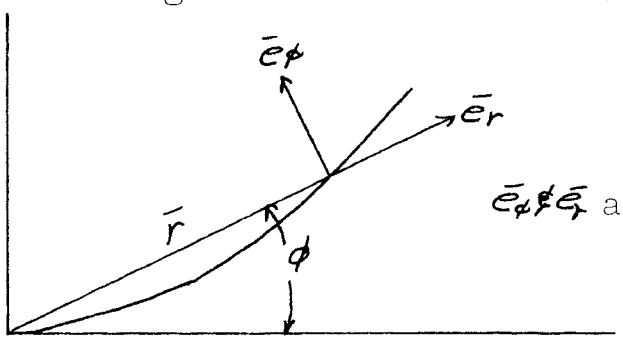

$\bar{e}_\phi$ & $\bar{e}_r$ are unit vectors

Figure AI-2, Polar Coordinates

*See reference[1]

Since the vector $\bar{r}$ is r units long in the $\bar{e}_r$ direction,

$$\bar{r} = r\bar{e}_r \tag{A1-1}$$

and the velocity is given by

$$\bar{V} = \dot{\bar{r}} = \dot{r}\bar{e}_r + r\dot{\bar{e}}_r \tag{A1-2}$$

where

$$\dot{\bar{e}}_r = \frac{d\bar{e}_r}{dt}$$

The unit vectors $\dot{\bar{e}}_r$ and $\dot{\bar{e}}_\phi$ must be determined. To do this we move from point P to point Q in Figure A1-3,

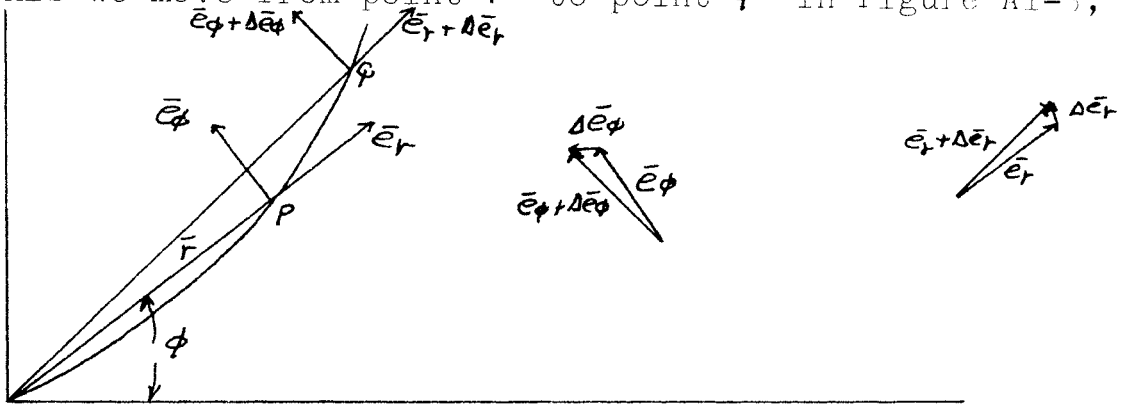

FIGURE AI-3

Evaluation of Polar Coordinate Unit Vectors

now in the limit

$$\dot{\bar{e}}_r = \frac{d\bar{e}_r}{dt}\frac{d\phi}{dt} = \dot{\phi}\bar{e}_\phi \tag{A1-3}$$

$$\dot{\bar{e}}_\phi = \frac{d\bar{e}_\phi}{dt}\frac{d\phi}{dt} = -\dot{\phi}\bar{e}_r \tag{A1-4}$$

the velocity vector may be written from A1-2-3-4 as

$$\bar{V} = \dot{r}\bar{e}_r + r\dot{\phi}\bar{e}_\phi \tag{A1-5}$$

The velocity for the geometry in Figure A1-1 is given as

$$\bar{V} = \dot{r} + r\dot{\phi} \qquad \text{(A1-6)}$$

where $\dot{r}$ is the velocity component taken in direction of r and $r\dot{\phi}$ is the component taken in the direction normal to r.

Then $$\dot{r} = V_t \cos\phi - V_M \cos(\phi - \phi_M) \qquad \text{(A1-7)}$$

and using the sign convention adopted in Figure A1-3

$$r\dot{\phi} = -V_T \sin\phi + V_M \sin(\phi - \phi_M) \qquad \text{(A1-8)}$$

and

$$\dot{\phi}_M = a\dot{\phi} \qquad \text{(A1-9)}$$

where (A1-9) represents the proportional mentioned in the definition where the constant a is called the navigation constant or the navigational correction. Now (A1-9) can be integrated directly and the result is

$$\phi_M = a\phi + \phi_0 \qquad \text{(A1-10)}$$

From reference [1] if $a=1$ and $\phi_0=\phi$, a pure pursuit course results, and if $a=1$ and ϕ_0 is fixed then a deviated pursuit course results. If $\dot{\phi} = 0$, we have a constant-bearing course. This was the reason for selecting this guidance mode as it is representative of various guidance schemes.

The equations of motion A7-8-9 cannot be solved in closed form except when $q = 2$. The solution for $q = 2$ can be found in reference [1] along with additional discussions of the dynamic characteristics of the proportional navigation scheme.

B-FAR FIELD CRITERION FOR PLANE WAVE

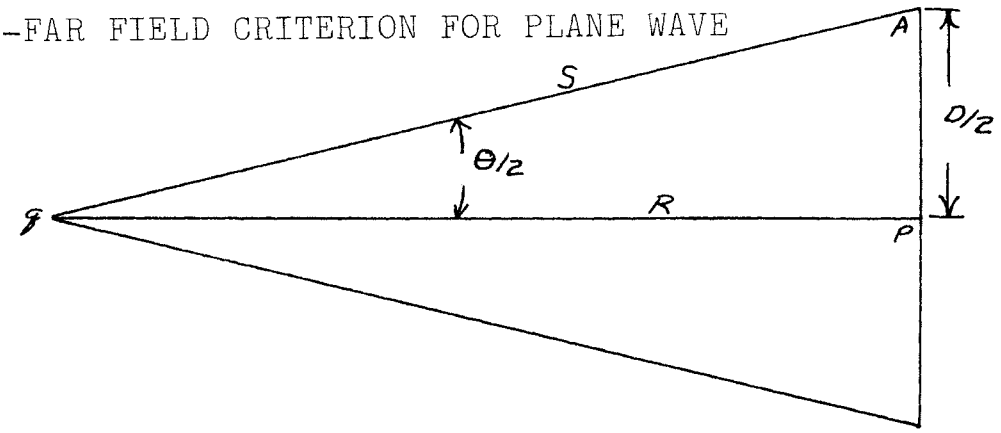

Figure AII-1, Antenna Pattern Geometry

A general criterion for the incident plane wave criterion can be found in Chapter 6, of reference 9. The development is based on the principles of optics. From Figure AII-1, an examination of the geometry reveals that for large R and a finite receiving aperature the phase variation across the aperature is zero, i.e., a plane wave.

For point P, a wave emitted from the source q will have a phase shift $\left(\frac{2\pi}{\lambda}\right)R$ and for the same wave arriving at A the phase shift will be $\left(\frac{2\pi}{\lambda}\right)S$. However, S is dependent on the range R and the aperature width D, since $S = [R^2 + D^2/4]^{1/2}$

Therefore the phase difference between P and A due to a wave traveling from q is, $\frac{2\pi}{\lambda}(S-R) = \Delta\phi$

or $$\frac{2\pi}{\lambda}\left[(R^2 + D^2/4)^{1/2} - R\right] = \Delta\phi$$

$$\omega(x,y) = \frac{1}{\pi n \sigma_0} e^{-(x^2+y^2)/n\sigma_0} \tag{3-37}$$

changing from rectangular coordinates (x,y) to polar coordinates (E,θ), the distribution becomes

$$\omega(E,\theta) = \frac{E}{\pi n \sigma_0} e^{-E^2/n\sigma_0} \tag{3-38}$$

Now if this expression is integrated with respect to θ,

$$\omega(E) = \frac{2E}{n\sigma_0} e^{-E^2/n\sigma_0} \tag{3-39}$$

and since $\sigma = x^2+y^2$, we have $(\sigma = E^2)$

$$\omega(\sigma)d\sigma = \frac{d\sigma}{n\sigma_0} e^{-\sigma/n\sigma_0} \tag{3-40}$$

This is the Rayleigh distribution, where the average cross section is $\bar{\sigma} = n\sigma_0$. Therefore, the average echoing area of the assembly is the sum of the echoing areas of the individual elements. Now, two glint models are available for continued analysis. From Barton (reference [3]) the power density for a standard glint model is,

$$\Phi(\omega) = \Phi(0) \frac{\omega_g^2}{\omega_g^2+\omega^2} \tag{3-41}$$

where Wg is the half-power frequency (noise bandwidth)

$$f_{MAX} = \frac{2\omega_a L}{\lambda} \tag{3-42}$$

(3)

and $\Phi(0)$ = is the zero frequency spectral density or average amplitude squared.

ω_a = rate of change of aspect angle

L = maximum dimension of the target measured normal to the direction of the radar beam and to the axis of rotation

λ = radar wave length

A second expression can be derived by translating the developed model into spectrum form. To calculate the power spectral density,

$$\Phi(\omega) = \int_{-\infty}^{\infty} e^{-j\omega\tau} R C\tau \, d\tau$$

where, $RC\tau = Ae^{-A\tau} d\tau$ (Rayleigh Power Distribution)

and, $A = 1/n\sigma_0$

Then
$$\Phi(\omega) = A\int_{-\infty}^{\infty} e^{-j\omega\tau} e^{-A\tau} d\tau$$
$$= A\int_{-\infty}^{\infty} (\cos\omega\tau - j\sin\omega\tau) e^{-A\tau} d\tau$$
$$= A\int_{-\infty}^{\infty} \cos\omega\tau e^{-A\tau} d\tau - Aj\int_{-\infty}^{\infty} \sin\omega\tau e^{-A\tau} d\tau$$

Returning to equation (3-42), and assuming that $RC\tau$ represents the autocorrelation function (which by definition is an even function).

Then $R(\tau) = Ae^{-A\tau}$

and
$$\Phi(\omega) = 2A\int_{0}^{\infty} e^{-A\tau} \cos\omega\tau \, d\tau \qquad (3\text{-}43)$$
$$= 2A\left\{\mathcal{L}[\cos\omega t]\right\}_{s=\beta} = \frac{2AB}{\omega^2 + B^2}$$

From the previous development, and the model described one observes that the glint spectrum is of the low-pass type, and from Barton, reference [3], the bandwidth is proportional to the spread in radial velocities within the target, divided by the radar wavelength (i.e., $\omega_g = 2\pi\left(\frac{2\omega_a L}{\lambda}\right)$). The general glint spectral density is demonstrated in figure III-5.

B-FAR FIELD CRITERION FOR PLANE WAVE

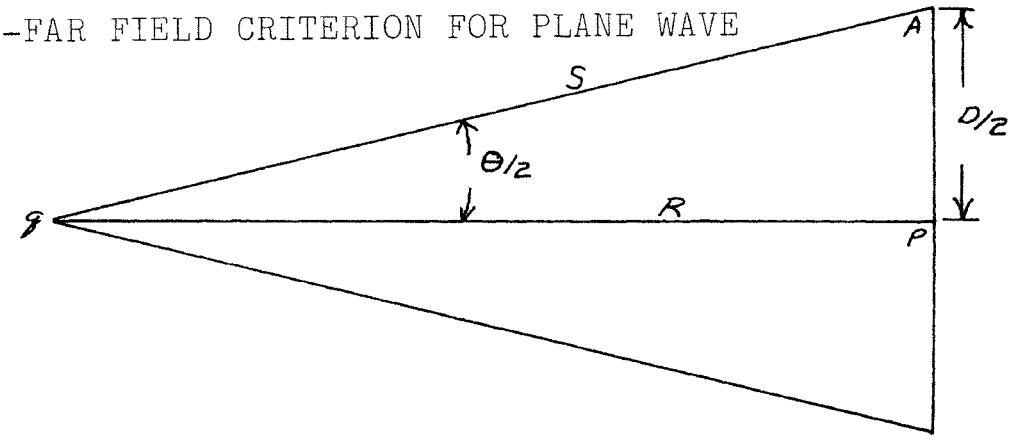

Figure AII-1, Antenna Pattern Geometry

A general criterion for the incident plane wave criterion can be found in Chapter 6, of reference 9. The development is based on the principles of optics. From Figure AII-1, an examination of the geometry reveals that for large R and a finite receiving aperature the phase variation across the aperature is zero, i.e., a plane wave.

For point P, a wave emitted from the source q will have a phase shift $\left(\frac{2\pi}{\lambda}\right)R$ and for the same wave arriving at A the phase shift will be $\left(\frac{2\pi}{\lambda}\right)S$. However, S is dependent on the range R and the aperature width D, since $S = [R^2 + D^2/4]^{1/2}$

Therefore the phase difference between P and A due to a wave traveling from q is, $\frac{2\pi}{\lambda}(S-R) = \Delta\phi$

or $$\frac{2\pi}{\lambda}\left[(R^2 + D^2/4)^{1/2} - R\right] = \Delta\phi$$

now assume

$$D/2 = KR, \quad K = D/2R, \quad R = D/2K$$

then

$$2\pi/\lambda\left[(R^2+K^2R^2)^{1/2}-R\right] = \Delta\phi$$

and

$$2\pi/\lambda\, R\left[(1+K^2)^{1/2}-1\right] = \Delta\phi$$

expanding the radical using the binomial theorem and disregarding higher order terms,

$$\Delta\phi = \frac{2\pi}{\lambda}\cdot\frac{RK^2}{2}$$

now
$$\Delta\phi = \frac{2\pi}{\lambda}\left(1+\tfrac{1}{2}K^2-1\right)R$$

$$\Delta\phi = \frac{2\pi}{\lambda}\left(\frac{K^2R}{2}\right)$$

now an accepted minimum phase shift is

$\lambda/16$ then $\frac{K^2R}{2} \leq \lambda/16$

and $K^2 \leq 2\lambda/16R = \lambda/8R$

and from the previous assumption,

$$K^2 \leq 2\lambda/16R = \lambda/8R = D^2/4R^2$$

or

$$R \geq 2D^2/\lambda$$

The problem which exists when considering a plane incident wave for glint analysis is that the target completely fills the seeker beamwidth and for a closing seeker the incident wave will not be a plane wave. For a purely analytic analysis this factor would have to be incorporated into the analysis, and this

technique used in the analysis of a two and three element target. The statistical approach could be handled by employing a two dimensional statistical model, however, the phase distortion in the incident wave along the target (aperture) will be incorporated as part of the random phase distribution returning from the target. Therefore, a constant-phase front is assumed for the incident wave at the target.

C-ANGULAR ERROR FOR THE TWO-ELEMENT TARGET

For the purposes of completing the analysis an expression will be developed for the angular error of a two-element target. The development will be similar to the approach used in reference [3] pages 85 through 89.

For the purposes of the development refer to figure AIII-1.

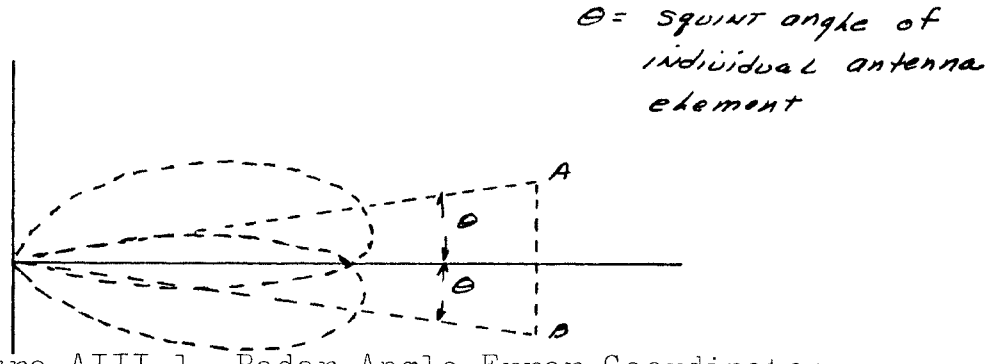

Figure AIII-1, Radar Angle Error Coordinates (One Coordinate)

For a simultaneous lobing radar, the angle error is derived by comparing the difference in the two received channels (for one coordinate) with the composite energy received (or the sum of the total return energy received). The voltage derived from each lobe is passed through an amplifier, detected, and then the difference is used to obtain the error

by dividing the difference by the sum. The sum channel providing a means for calibrating the error channels for varying target positions relative to the antenna line-of-sight.

Now again referring to Figure AIII-1, the boresight axis is directed at the center of the target AB, and for a small angular displacement, the slope of the antenna lobes can be considered constant, and will be denoted by g.

$\bar{E}_A$ and $\bar{E}_B$ represent the received voltages from the target when $\theta=0$, and their phase difference is given by ϕ.

The total RF voltage received by the upper lobe is,

$$E_u = E_A(1+g\theta) + E_B(1-g\theta)e^{j\phi} \qquad \text{(A3-1)}$$

and for the lower lobe,

$$E_L = E_A(1-g\theta) + E_B(1+g\theta)e^{j\phi} \qquad \text{(A3-2)}$$

the difference voltage is

$$E_D = K\left(|E_u|^2 - |E_L|^2\right) \qquad \text{(A3-3)}$$

and substituting A3-12 into A3-3 and simplifying

$$E_D = K4g\theta\left[E_A^2 - E_B^2\right] \qquad \text{(A3-4)}$$

where K = amplifier gain, the sum channel is

$$E_S = K\left(|E_u|^2 + |E_L|^2\right) \qquad \text{(A3-5)}$$

which simplifies to,

$$E_S \cong 2K\left[E_A^2 + E_B^2 + 2E_AE_B\cos\phi\right] \qquad \text{(A3-6)}$$

the error voltage as previously defined is the ratio of the difference and the sum signals or,

$$\frac{E_D}{E_S} = \frac{4K^2 g(\theta)[E_A^2 - E_B^2]}{2K[E_A^2 + E_B^2 + 2E_A E_B \cos\phi]} \qquad (A3\text{-}7)$$

now for a single target,

$$\frac{E_D'}{E_S} = \frac{4K^2 g\theta E_A^2}{2KE_A^2} = 2g\theta \qquad (A3\text{-}8)$$

Therefore the apparent shift (error) at the boreshight angle for a two-element would be

$$\frac{\frac{E_D}{E_S}}{\frac{E_D'}{E_S}} = \frac{2g\theta(E_A^2 - E_B^2)/(E_A^2 + E_B^2 + 2E_A E_B \cos\phi)}{2g\theta}$$

or substituting θ' for E_D/E_S and $\theta = E_D'/E_S$

$$\theta' = \frac{\theta[1 - (E_B/E_A)^2]}{1 + (E_B/E_A)^2 + 2E_B/E_A \cos\phi} \qquad (A3\text{-}9)$$

Now, a relationship between the angle off-set θ and the relative phase relationship ϕ is required.

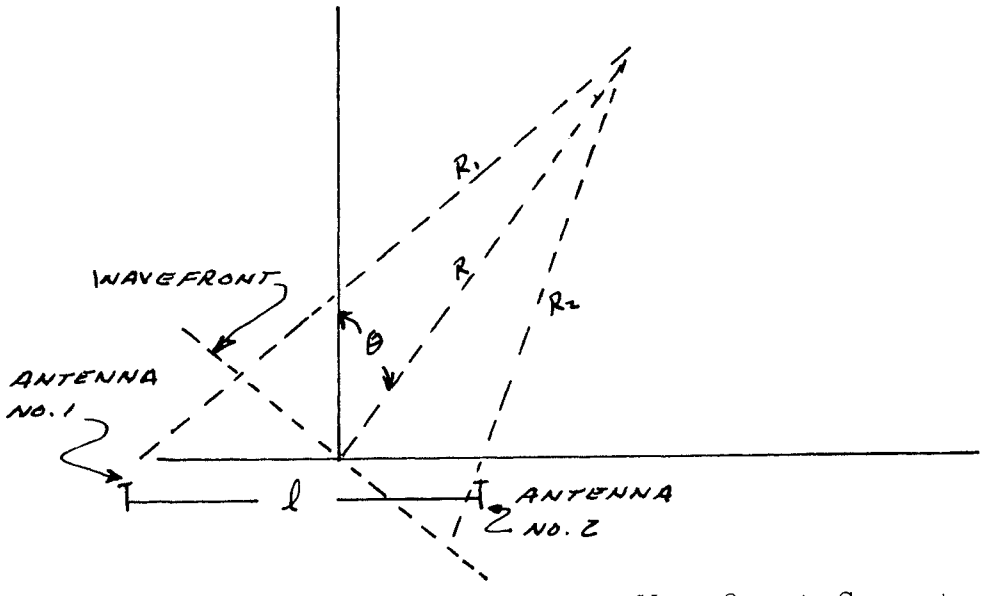

Figure AIII-2, Wavefront Geometry

From figure AIII-2,

$$R_2 = R - \ell/2 \sin\phi \qquad \text{(A3-10)}$$

$$R_1 = R + \ell/2 \sin\phi \qquad \text{(A3-11)}$$

Now for a reflecting target, the total phase difference is given by,

$$\Delta\phi = \frac{4\pi}{\lambda}(R_1 - R_2)$$

and

$$R_1 - R_2 = R + \ell/2 \sin\phi - (R - \ell/2 \sin\phi)$$

$$= \ell \sin\phi$$

Therefore

$$\Delta\phi = \frac{4\pi}{\lambda} \ell \sin\phi \qquad \text{(A3-12)}$$

and,

$$\tan\Theta = \ell/2 / R\cos\phi$$

For small angles, $\sin\Theta \cong \Theta$ (in radians)

therefore*

$$\Theta = \frac{\ell \cos\phi}{2R}$$

$$\Theta' = \frac{\ell\cos\phi}{2R} \frac{1-K^2}{1+K^2+2K\cos\phi} \qquad \text{(A3-13)}$$

where K is the ratio of echos from target A and B, and ℓ is the separation of the target elements, and ϕ is given by

$$\phi = \frac{4\pi\ell}{\lambda} \sin\phi$$

---

*For the purposes of this discussion the target major axis was assumed to be nearly perpendicular to the radar line-of-sight.

For the purposes of this analysis assume

$$K^2 \ll 1$$

$$\theta' \cong (\ell \cos\phi)/2R(1+2K\cos\phi)$$

$$\cong \frac{\ell \cos\phi}{R}/2(1+2K\cos\phi) \qquad \text{(A3-14)}$$

VIII. BIBLIOGRAPHY

(1) Locke, Arthur S. Guidance, D.Van Nostrand Co. Inc. 1955

(2) Povejsil, Raven, Waterman, Airborne Radar, D. Van Nostrand Co. Inc., 1961

(3) Barton, David K., Modern Radar Analysis, Prentice-Hall Inc., 1964

(4) Jordan, Edward C., Electromagnetic Waves and Radiating Systems, Prentice-Hall Inc., 1968

(5) Shinners, Stanley M., Control System Design, John Wiley & Sons, Inc., 1964

(6) Beckmann, Petr, Probability in Communication Engineering, Harcourt, Brace & World, Inc., 1967

(7) Pipes, Louis A., Applied Mathematics for Engineers and Physicists, McGraw-Hill, Inc., 1958

(8) James, Nichols, and Phillips, Theory of Servo-mechanisms, McGraw-Hill, 1947

(9) Silver, Samuel, Microwave Antenna Theory and Design, McGraw-Hill, 1947

(10) Schwartz, Mischa, Information Transmission, Modulation, and Noise, McGraw-Hill, 1959

(11) Truxal, John G., Automatic Feedback Control System Synthesis, McGraw-Hill, 1955

IX. VITA

Franklin Delano Hockett was born on April 17, 1933, in Des Moines, Iowa. He received his primary and secondary education in Des Moines, and Runnells, Iowa. He attended the State University of Iowa, Iowa City, Iowa, and received his Bachelor of Science Degree in Electrical Engineering during June, 1959.

While the author was employed at Collins Radio Co., Cedar Rapids, Iowa, he took graduate courses from Iowa State University, Ames, Iowa during the years 1962 - 64. He has been enrolled in the St. Louis Graduate Extension Center of the University of Missouri, at Rolla, since September 1964. During this time interval he has been employed at McDonnell-Douglas Corporation and more recently at Conductron-Missouri.